American Institute of Aeronautics and Astronautics 2011-2012 Undergraduate Individual Aircraft Design Competition Proposal

Alex Lopez

Instructor: Dr. Ron Barrett

THE UNIVERSITY OF KANSAS

Department of Aerospace Engineering

May 10, 2012

American Institute of Aeronautics and Astronautics 2011-2012 Undergraduate Individual Aircraft Design Competition Proposal

Intent Form
2011/2012
AIAA Foundation
Undergraduate Individual Aircraft Design Competition
Request for Proposal:
Unlimited Class Air Racer

Title of Design Proposal: _Preliminary Design of the Atlas RX_____

Name of School: _University of Kansas_____

Designer's Name	**AIAA Member #**	**Graduation Date**	**Degree**
_Alex Lopez ___	___302745___	__May 13, 2012 __	_Aerospace Engineering

E-mail

In order to be eligible for the 2011/2012 AIAA Foundation Undergraduate Individual Aircraft Design Competition, you must complete this form and return it to AIAA Student Programs ***before 19 March 2010***, at AIAA Headquarters, along with a one-page "Letter of Intent" as noted in Section III, "Schedule and Activity Sequences." For a nonmember, a student member application and member dues payment should also be included with this form.

1 Dec. 2011

_____
Signature of Faculty Advisor
Date

Signature of Project Advisor

Dr. Ron Barrett
1 Dec. 2011

Dr. Ron Barrett

___
Faculty Advisor – Printed
Date

Project Advisor – Printed

adaptivebarrett@yahoo.com

adaptivebarrett@yahoo.com

Faculty Advisor – Email

Project Advisor – Email

Table of Contents

List of Figures Page #

List of Tables

Page #

List of Symbols

Symbol	Description	Units
AMP	Airplane Market Price	USD
AR	Aspect Ratio	~
b	Wing Span	ft, in
b_t	Tire Base Width	in
BL	Butt Line	in
c	Chord	in
c_p	Specific Fuel Consumption	lb/hp-hr
$\bar{c}$.	Mean Geometric Chord	ft
C_D	Drag Coefficient	~
C_{D_o}	Zero Lift Drag Coefficient	~
c_f/c	Flap Chord to Wing Chord Ratio	~
c.g.	Center of Gravity	~
C_L	Lift Coefficient	~
C_M	Pithcing Moment Coefficient	1/rad
d_s	Strut Diameter	in
D	Drag	lbs
D_t	Tire Diameter	in
e	Oswald's Efficiency Number	~
FS	Fuselage Station	in
k_α	Feedback Gain	deg/deg
L	Lift	lbs
M	Mach Number	~
M_{ff}	Mission Fuel Fraction	~
P	Power	hp
R	Range	nmi
R_{turn}	Turn Radius	ft
s	Strut	~
s_s	Strut Stoke	in
S	Wing Area	ft^2
SHP	Shaft Horse Power	Hp
SM	Static Margin	%
S_{LG}	Landing Distance	ft
S_L	Landing Runway Distance	ft
t	Thickness	in
V	Volume	ft^3
VA	Volts-Amps	Volts-Amps
V_M	Maneuvering Velocity	knots
W	Weight	lbs
W_{crew}	Crew Weight	lbs
W_E	Empty Weight	lbs

List of Symbols (Continued)

Symbol	Description	Units
W_F	Fuel Weight	lbs
W_{TO}	Takeoff Weight	lbs
WL	Waterline	in
W/P	Power Loading	lbs/hp
$(W/P)_{TO}$	Takeoff Power Loading	lbs/hp
W/S	Wing Loading	lbs/hp
$(W/S)_{TO}$	Takeoff Wing Loading	lbs/hp
$\bar{x}$.	Distance Along X-Axis as a Fraction of $\bar{c}$.	~
X	Location along X Axis	ft
Y	Location along YAxis	ft
Z	Location along Z Axis	ft

List of Symbols (Continued)

Greek Symbols

Symbol	Description	Units
α	Angle of Attack	Degrees
Γ	Dihedral Angle	Degrees
δ	Deflection Angle	Degrees
δ_f	Flap Deflection Angle	Degrees
Δ	Change	~
ε	Wing Twist Angle	Degrees
η	Wing Station	%
θ	Angle	Degrees
ι	Incidence Angle	Degrees
λ	Taper Ratio	~
Λ	Sweep Angle	Degrees
ξ	Dampening Ratio	~
ξ_D	Dutch Roll Dampening Ratio	~
φ_{turn}	Turn Bank Angle	degrees
ω_n	Natural Frequency	rad/sec
$\omega_{n.D}$	Dutch Roll Natural Frequency	rad/sec

List of Symbols (Continued)

Subscript	Description	Units
a	Aileron	~
cg	Center of Gravity	~
c/4	Quarter Chord	~
dorsal	Dorsal Strake	~
e	Elevator	~
el	Electric	~
er	Elevator Root	~
et	Elevator Tip	~
extr	Extracted	~
f	Flap	~
fuel	Fuel	~
fus	Fuselage	~
gen	Generator	~
h	Horizontal Tail	~
hydr	Hydraulic	~
i	Inboard	~
long	Longitudinal	~
L	Landing	~
mech	Mechanical	~
mgc	Mean Geometric Chord	~
n	Gravity Loding	~
o	Outboard	~
P	Phugoid	~
r	Rudder	~
s	Stall	~
SP	Short Period	~
t	Tip	~
TO	Takeoff	~
v	Vertical Tail	~
ventral	Ventral Strake	~
w	Wing	~
wet	Wetter Area	~
wing fence	Wing Fence	~
wf	Wing with Flap	~
δ_f	Flap Deflection Angle	~

Acronyms

AAA	Advance Aircraft Analysis	~
AIAA	American Institute of Aeronautics and Astronautics	~
CAD	Computer Aided Design	~
HUD	Heads Up Display	~
LCD	Liquid Crystal Display	~
MGC	Mean Geometric Chord	~
NACA	National Advisory Committee for Aeronautics	~
NTSB	National Transportation Safety Board	~
RFP	Request For Proposal	~
UAV	Unmanned Arial Vehicle	~

Acknowledgment

The author would like to thank Dr. Barrett for his guidance during the process of this report. With his guidance the appropriate decisions were completed to direct the design of the Atlas RX to be a winning racer.

1 Validation Dataset, Method Calibration and Introduction

Given that most current Reno Air Race aircraft are out dated and old technology, it is time to for current technology in materials, electronics and new aircraft designs be brought to this field. With the implementation of advanced technology, computer software and a fresh mind, the Atlas RX is born. With its slick and streamline curves, employment of advance adaptive composite structures and overall visual appeal, the Atlas RX is this generations unlimited class Reno racer. With proven calculations, the Atlas RX will not only be competitive with other racers, but will leave them in its wake, with a max cruise velocity of 625 mph, which is more than 100 mph faster than any other aircraft in the unlimited class. With that said, here is the future of Reno's unlimited class aircraft.

Figure 1-1 Atlas RX

1.1 AIAA Request for Proposal

This section entails the information and regulations that is presented in the Request for Proposal, RFP, given by the American Institute of Aeronautics and Astronautics, AIAA, consisting of the mission specifications and profile. Presented below are the requirements from the RFP (ref. 1)

- Piston engine driven propeller only
- Turbo-charging will be allowed

- No turbo-compounding
- Pilot must be on board the aircraft, thus no UAV
- No deliberately cutting pylons
- Empty weight of at least 4500 lbs
- Capability of pulling 6 G's
- Be competitive with in the race mission at a speed equal to or greater than 500 mph
- Ferry capability of 500 nm
- Takeoff and landing performance appropriate for Stead Airfield, location of Reno Air Race.
- FAA Experimental certification basis

The following figure presented below is that of the race mission profile

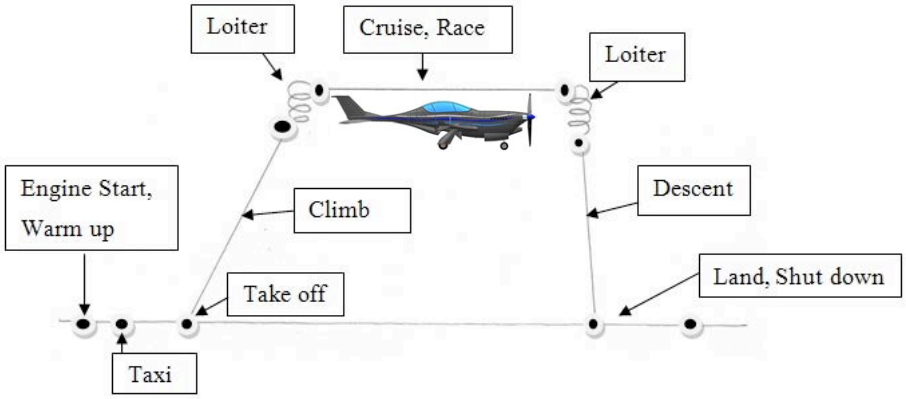

Figure 1-2: Race Mission Profile

The following figure presented below is that of the ferry mission profile.

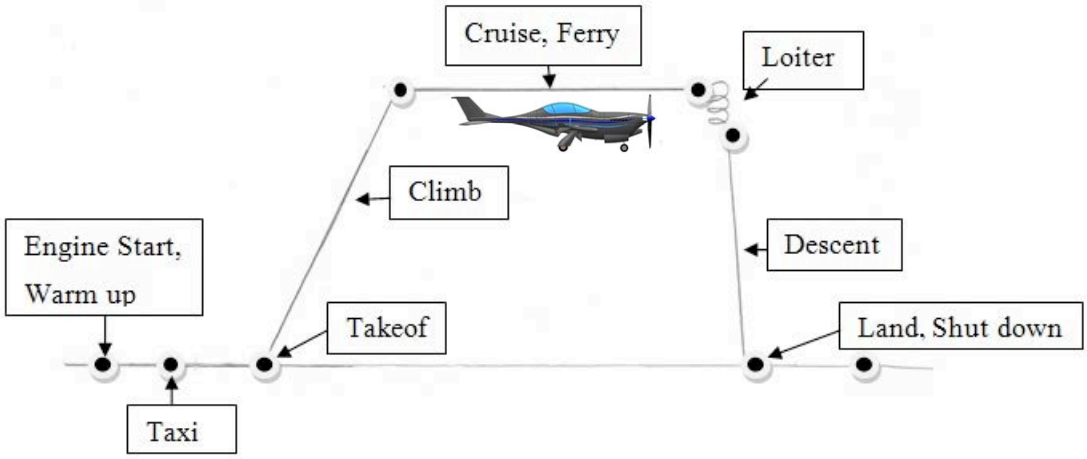

Figure 1-3: Ferry Mission Profile

1.2 Method of Calibration

The computer software programs that were used to generate measurements and calculations were as follows;

- NX v 7.5 for computer aided design, CAD (ref. 2)
- Advanced Aircraft Analysis (AAA) v 3.2 for calculation (ref. 3)

NX[2], being that it is a highly reputable software program; all measurements taken from the CAD file are reliable and accurate.

AAA[3] was used for all calculations involving surface plan forms, lift and drag analysis as well as all stability and control, as well as many others.

2 Design Justification & Technical Approach to Meet Mission Requirements

2.1 Fly Low, Go Fast and Turn Left

The saying "Go fast and turn left" is a motto by which all Reno Air Race pilots fly by. Keeping the same standard of flying, the Atlas RX will employ similar methods increasing max cruise velocity.

Current racers, such as Team Voodoo[4], Team Dago Red[5] and Team Rare Bear[6], take an existing aircraft and modify it to achieve desired flight conditions. One of the methods that these teams employ is shortening wing span. As seen from the Galloping Ghost[7], this can have catastrophic out comes. Instead, the Atlas RX will use a properly sized wing that is smaller than traditional racers, but not by shortening the span, however; shortening the chord of the wing.

Figure 2-1: Team Voodoo[4], Team Dago Red[5] and Team Rare Bear[6]

As a result of this, a higher wing loading is achieved from a smaller wing area. As this will be discussed in later sections, to achieve a proper aspect ratio, AR, the mean geometric chord, mgc, is sized given the proper calculated wing area, S_w. It is found that that a smaller chord is beneficial allowing for a high AR and thus a lower required horse power, Hp_{req}.

In addition to smaller wing area, a small total wetted area, $S_{wet,total}$, compared to the current Reno racers, will allow for higher cruise speeds. This is achieved by "slimming down" the fuselage to only the required volume. By designing the outer curves of the fuselage to "hug" the pilot and engine, one is able to achieve the smallest possible fuselage.

2.2 Safety

It is known that safety by all measures is the most important issue of concern when designing a Reno Air Race aircraft that will be flying so close to spectators. Some of the safety features that the Atlas RX will employ are the following.

- Martin Baker ejection seat
- Canopy jettison system
- High impact resistant canopy
- Kevlar wing leading edge
- Self-sealing fuel tanks
- Internal fire extinguisher system
- Ground proximity sensors
- LCD display of surrounding object
- Heads up display (HUD) of insightful flight data
- Triple redundant flight control system
- Scimitar Propeller
- Engine Cooling
- Use of known and reliable products

The pilot of the atlas will be seated in a Martin Baker US16E-JSF ejection seat (ref. 8). Known for its reliability and saving lives of US combat pilots, this ejection seat is designed for high ejection speeds, 600 KEAS. Prior to ejecting from the aircraft the canopy will clear the pilots' head with the use of a similarly common canopy jettison system used in F-16.

Figure 2-2: Martin Baker US16E-JSF Ejection Seat (ref. 8)

Due to the relatively low race altitude of the aircraft, bird strikes are of concern. To prevent any hazardous object from penetrating the aircraft or the canopy itself, high impact resistant glass, much like the current canopy glass used on today's joint strike fighters, will be used to protect the pilot from any obstructions. In addition, a Kevlar wing leading edge will be implemented to protect from any objects puncturing the fuel tanks.

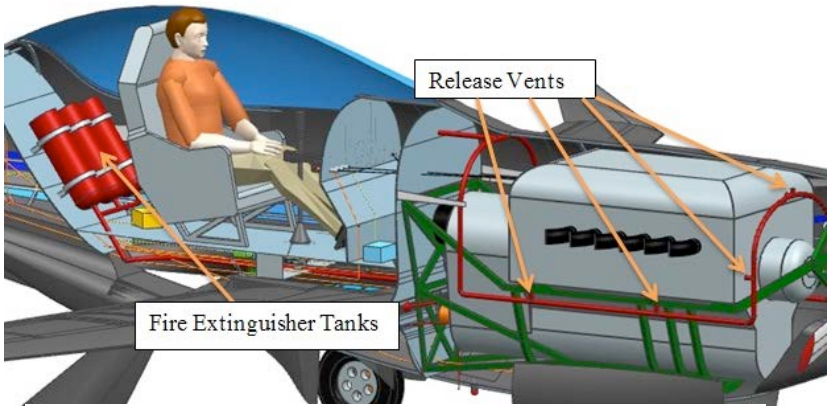

Figure 2-3: Fire Extinguisher System

If there should arise any issue that the wings be torn apart, the fuel tanks will be self-sealing, thus not allowing the chance for any ignition of the fuel.

Many recall of the famous Burt Rutan Pond Racer and the catastrophic cause of its demise. To subdue any in fires in

flight, an on board Halon fire extinguisher system will be used and directed towards that engine bay.

While racing around the pylons at Stead Field, the worst possibility of a crash would be that of an aircraft flying into the stands, as one saw in the 2011 Reno Air Races. To prevent this from ever happening again a ground proximity sensor will be used. Prior to the race a minimum altitude can be set for race conditions, simply put, the aircraft will not be allowed to fly below this set altitude or 'hard deck' when this system is active. If for whatever reason the aircraft should drop below this so called 'hard deck' this system will be able to override the pilots' control and bring the aircraft to a safe altitude. Shown in the figure on can see the appropriate placement of the ground proximity sensors and the sweeping area.

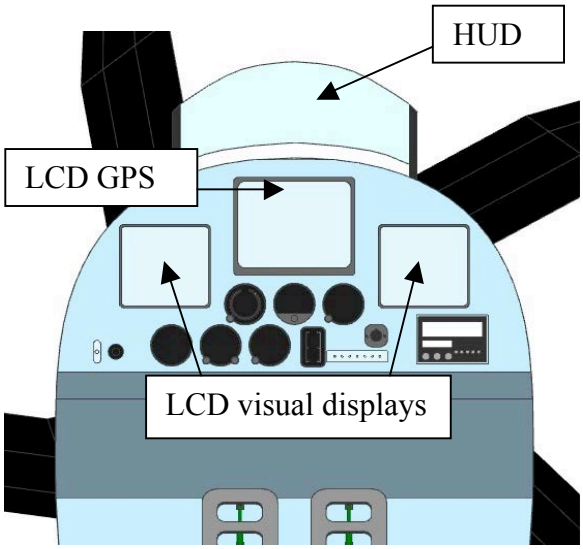

Figure 2-4: Visual Systems, LCD Displays and HUD

To avoid mid-air collisions two heads up LCD displays with in the cockpit will allow for the pilot to view 360 degrees around all axes and any aircraft with in close proximity of the Atlas RX. This will allow for the pilot to make safe judgments to flight path of the Atlas RX.

From National Transportation Safety Board (NTSB) of the galloping ghost, and talking with current Reno pilots, relieving some of the duties of the pilot must be taken into consideration. Thus a HUD will be used to display pertinent flight data. By allowing the pilot to focus on just flying the aircraft and looking what's ahead of them, the stress level of the pilot can be reduced. In addition, automatic triggering such as landing gear retraction once the aircraft has reached a flight level of 50 ft after takeoff, also auto propeller feathering during an engine out situation. More of these auto triggering sequences will be discussed later in the report.

Further explained within the system section of this report, the Atlas RX flight control system is that of a triple redundant irreversible system. Having the redundancy of three independent systems ensures that proper signals are seen from the pilots command.

To reduce propeller tip speed a scimitar propeller, much like the one used on the Airbus 400, will be used. By sweeping the blades of the propeller higher tip speed can be achieved without suffering from Mach and compressibility effects.

Finally, using known reliable products will add to the safety of the Atlas RX, one example being the engine. Used by many of the competitors currently in the unlimited class of the Reno Air Races, a variation of the Rolls Royce Merlin V-1650 will be the power house for the Atlas RX. The canopy, as mentioned previously will be similar to that of current canopies used on

joint strike fighters in service today. The ejection seat, a trusted Martin Baker US16E-JSF ejection seat, and artificial vision through the use of the two heads up LCD displays, which are already used in racing aircraft today, much like the Nemesis NXT. Finally, the radiator will be similar to that of the P-51 mustang. Although smaller than a full scale mustang, one can still trust its reliability and the expected thrust increase.

3 Class I & Class II Sizing Methods and Sensitivities

3.1 Configuration Considerations

3.1.1 Overall Configuration

Based on the information from the RFP, one was able to conclude that the Atlas Rx would be that of conventional (tail aft) based aircraft.
Reasoning for these decisions are as follows:

- RFP states that the Atlas RX must take off from the current runway that is on location at the Reno Air Race airport, Stead Field, thus water based or amphibious aircraft would not be required.
- Conventional aircraft configurations have more readily available information than other configurations
- Both land based and Conventional configurations will save cost.

Figure 3-1: Stead Field, Reno Nevada (ref. 9)

3.1.2 Wing Configuration

A joined wing, flying wing and oblique wing configurations were not used due to a significant amount in complexity and feasibility.

As seen from the research that was completed in Reference 10, the most common configuration is that of a low wing aircraft. From the research it was concluded that the Atlas RX would be a low wing aircraft.

3.1.3 Fuselage Configuration

The fuselage configuration for the Atlas RX is conventional. The reasoning for this is as follows:

- Allows for a forward mounted single engine configuration
- Light configuration

3.1.4 Empennage Configuration

The empennage configuration for the Atlas Rx will be that of a conventional configuration with the vertical stabilizers mounted to the aft of the fuselage. However; the horizontal stabilizer will be mounted to the tip of vertical stabilizer allowing for a smaller

vertical tail area, S_V, as this configuration increases the effectiveness of the vertical tail. Even further, the vertical tail will have a dorsal strake to assist with vortices adhering to its surface thus increasing its effectiveness and decreasing S_V.

3.1.5 Engine Configuration

The engine configuration will be that of a single engine in a tractor (pulling) formation turbo-charged piston/prop as defined by the RFP. This will allow for the engines' propeller to be in "clean air" compared to a pusher configuration were the prop will see perturbed flow from the body of the aircraft. In addition, risk of catastrophe and unstable flying conditions increase as the number on engines increase.

3.1.6 Landing Gear Configuration

When deciding the land gear configuration for the Atlas RX, one looked at the pros and cons for both tail dragger and tricycle gear configurations. These are presented in table below.

Table 3-1: Landing Gear Configuration Pro's and Con's

	Pros	Cons
Tail dragger	➢ Great for prop clearance ➢ Will allow for landing gear storage in wings	➢ Possibility of ground looping ➢ High risk of tip-over ➢ Poor ground visibility
Tricycle	➢ Will allow for landing gear storage in wings or fuselage ➢ Great ground visibility ➢ Low risk of tip-over	➢ Prop/ground clearance is limited for large props

After this, one decided that the Atlas RX would be that of a retractable tricycle configuration, as prop/ground clearance was found to be negligible.

The following concludes the configuration for the Atlas RX.

Table 3-2: Atlas RX Configuration

Configuration	Description
Overall	Land based conventional
Wing	Low wing
Fuselage	Conventional
Empennage	Conventional vertical and horizontal T-tail configuration
Engine	Tractor buried in the front of the fuselage
Landing Gear	Retractable tricycle

3.2 Class I Sizing

Shown in the figure below one can see the preliminary sizing plot generated from AAA[3].

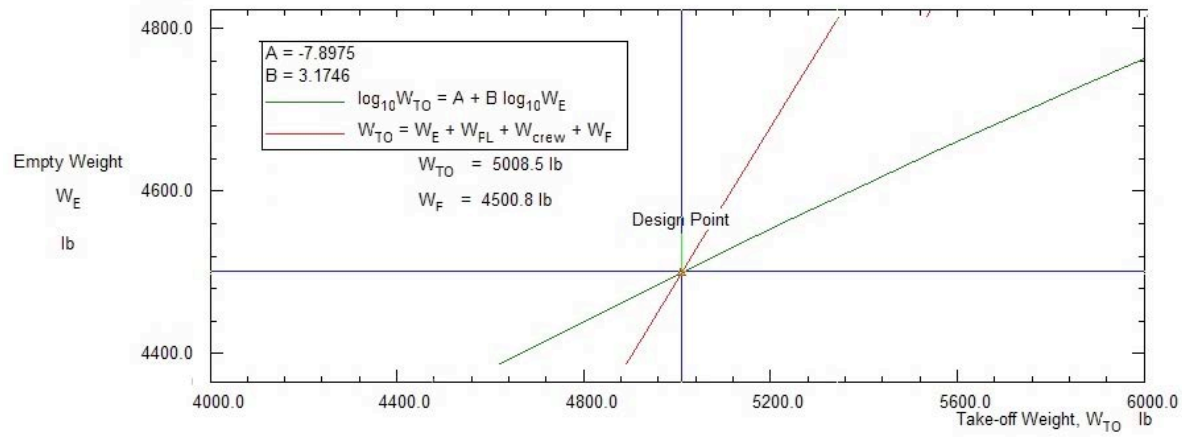

Figure 3-2: Sizing Plot AAA[3]

Once the takeoff weight is determined, the sensitivities due to various parameters were calculated. It seen that the aircraft is highly sensitive to lift to drag ratio, L/D, thus the aircraft was sized for an L/D of 10 with a specific fuel consumption, c_p, of .9 lb/hr/hp.

Following this a matching plot based on flight conditions is generated as seen in the figure on the next page.

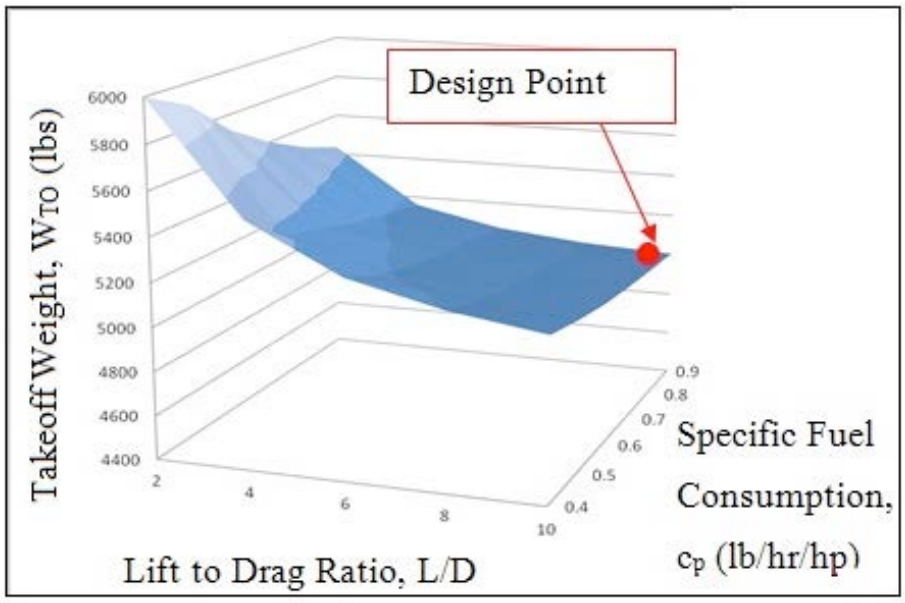

Figure 3-3: Sensitivity Plot; Takeoff Weight, W_{TO} vs. Lift to Drag Ratio, L/D vs. Specific Fuel Consumption, c_p

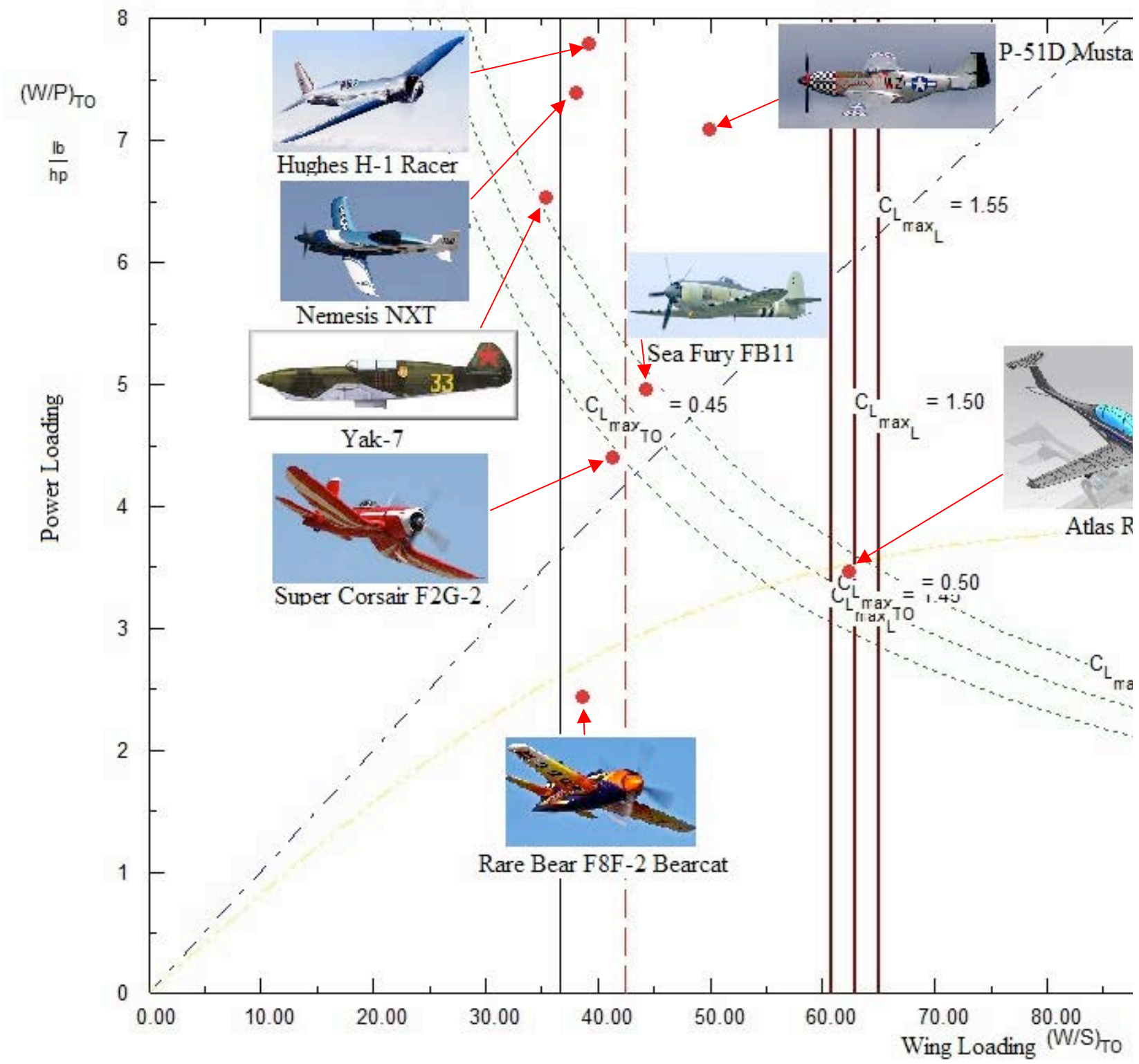
$(W/P)_{TO}$
lb/hp
Power Loading
Wing Loading $(W/S)_{TO}$
0.00
10.00
20.00
30.00
40.00
50.00
60.00
70.00
80.00
0
1
2
3
4
5
6
7
8
Hughes H-1 Racer
Nemesis NXT
Yak-7
Super Corsair F2G-2
Rare Bear F8F-2 Bearcat
Sea Fury FB11
P-51D Musta
Atlas R
$C_{L_{max_L}} = 1.55$
$C_{L_{max_{TO}}} = 0.45$
$C_{L_{max_L}} = 1.50$
$C_{L_{max_{TO}}} = 0.50$

As mention previously, as opposed to shortening the span of the wing, the Atlas RX will have a smaller mgc. Due to the desired flight speeds of the Atlas RX, 500 knots, super critical airfoils will be used for all surfaces as the aircraft will be in the transonic region. To compensate for drag divergence Mach number, M_{DD}, NASA Report, Reference 11, were used. From these the proper thickness to chord ratio, t/c, the wing is sized. It is seen from the figures shown below, that the proper t/c, of the wing is 14.5, given a flight Mack number of 0.76.

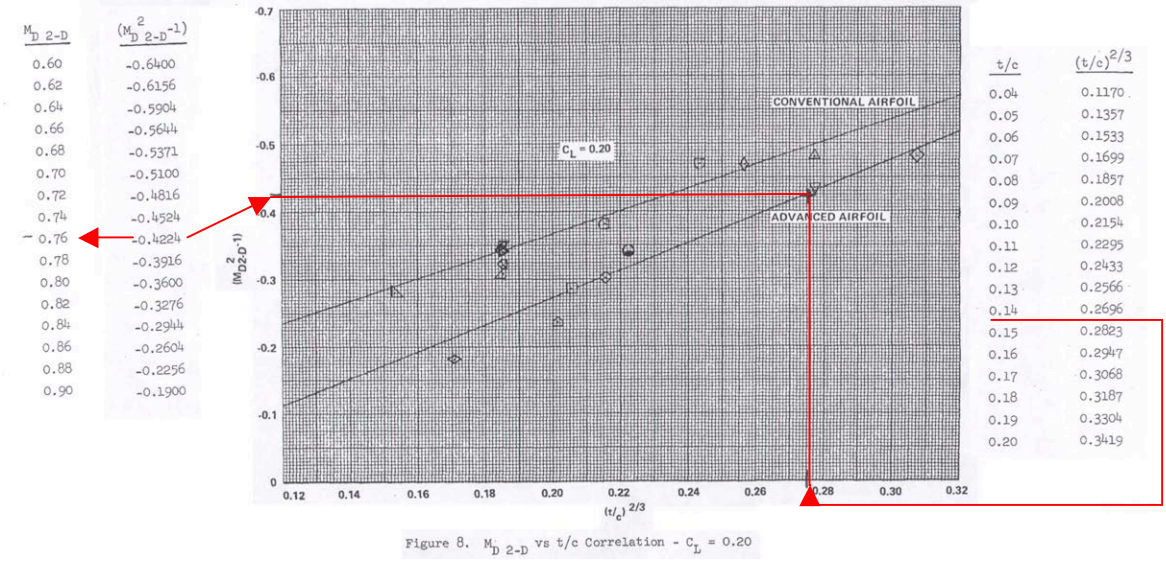

Figure 3-5: Drag Divergence Mach number vs. Thickness to Chord Ratio (ref. 11)

As this t/c is larger than desired, the wing will be swept, thus allowing for a lower t/c. Shown in the figure below one can see the proper correction for t/c due to sweep angle.

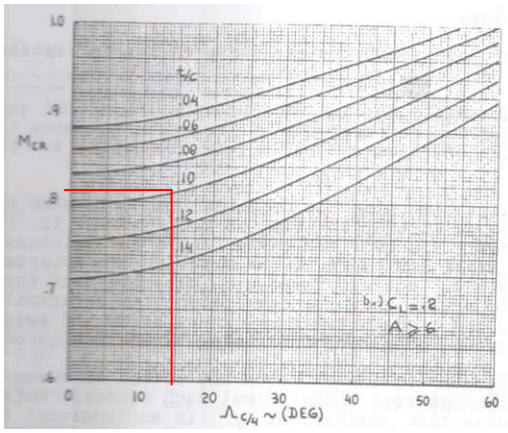

Figure 3-6: Thickness to Chord Ratio, t/c Correlation to Quarter Chord Sweep Angle, $\Lambda_{c/4}$ (ref. 12)

3.3 Class I Sizing

3.3.1 Engine Sizing

From Figure 3-4: Matching Plot AAA[3], the required horsepower for the Atlas RX is 1430 hp. It was decided to use a known and reliable engine, one that parts can still be found for and thus a Rolls Royce Merlin engine will be used. Given that current Reno competitors use the same engine, the true advantage to using this engine will be that the Atlas RX has a lighter takeoff weight as well as smaller wetted area, resulting in a higher cruise velocity. Normally the Merlin is a supper charged engine, as this is not permitted by the RFP, a modification to the engine will be done to allow for a turbo-charger. Shown in the table below one can see the engine specifications.

Table 3-3: Rolls Royce Merlin Engine Specifications (ref. 13)

Parameter	Value
Type	12-cylender
Bore	5.4 in
Stroke	6 in
Displacement	1,650 in^3
Length	88.7 in
Height	30.8 in
Width	40 in
Dry Weight	1,640 lb

3.3.2 Wing Sizing

From the sizing plots previously presented, the wing area is found to be 81 ft^2, shown in the figure one can see the plan form of the wing half.

The Atlas RX uses a cranked wing to provide a greater volume for landing gear storage. Had this not been done the main landing gear tire would have not been able to be completely stowed away within the wing. Shown in the following table one can see the wing geometric characteristics.

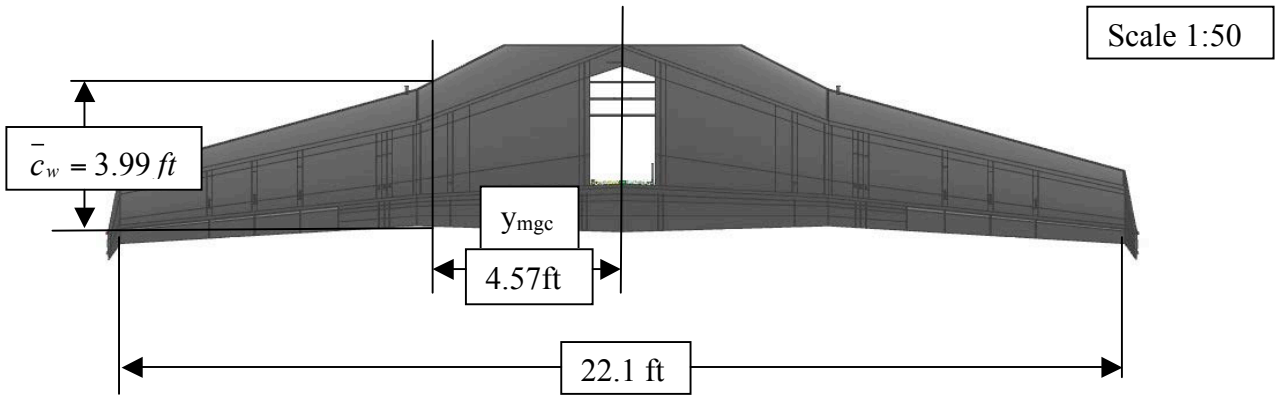

Figure 3-7: Atlas RX Wing

Table 3-4: Wing Geometric Characteristics

Parameter	Value
Quarter chord sweep angle, $\Lambda_{c/4}$	15.5 degrees
Aspect Ratio, AR	6
Thickness ratio, t/c	10%
Taper ratio, λ	0.32
Incidence, i_w	2.00 degrees
Dihedral, Γ	2.8 degrees
Wing wash-out, ε_w	-3.00 degrees
Wing area, S_w	81 ft^2
Airfoil	NACA 66-210

To assist with $C_{l\beta}$, wing fences were added to the wing tips as all side forces are equalized compared to a simple winglet configuration. Shown in the figure one can see the wing fences.

The wing fences were sized under the following criteria; acting as side force generators, SFG, as well as pilot's visibility. While banking around the pylons, the wing fences will act as wings, generating lift for the aircraft to have greater stability in addition the wing fences were sized to provide minimal obstruction of view for the pilot. Shown in the table below one can see the wing fence geometric characteristics.

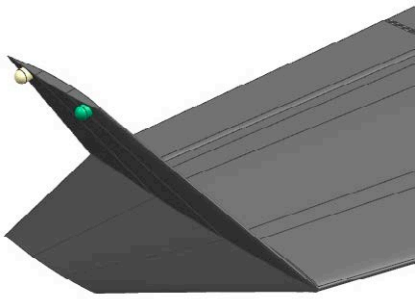

Figure 3-8: Wing Fence

Table 3-5: Wing Fence Geometric Characteristics

Parameter	Value
Quarter chord sweep angle, $\Lambda_{c/4}$	26.8 degrees
Aspect Ratio, AR	.484
Thickness ratio, t/c	10%
Taper ratio, λ	.41
Dihedral, Γ	± 65 degrees
Area, S	.807ft^2 per half
Airfoil	NACA 66-210

3.3.2.1 Aileron and Flap Sizing

It was decided that the flaps of the Atlas RX would be a split flap configuration. As this increases drag, the flaps themselves would act as speed breaks and allow for the aircraft to land at reasonable speeds. From sizing the flaps, the ailerons where assumed to have the same

chord, simply extending from the tip of the flap to the tip of the wing, the ailerons were sized. Shown in the following figure one can see the flaps and ailerons on the equivalent wing plan form.

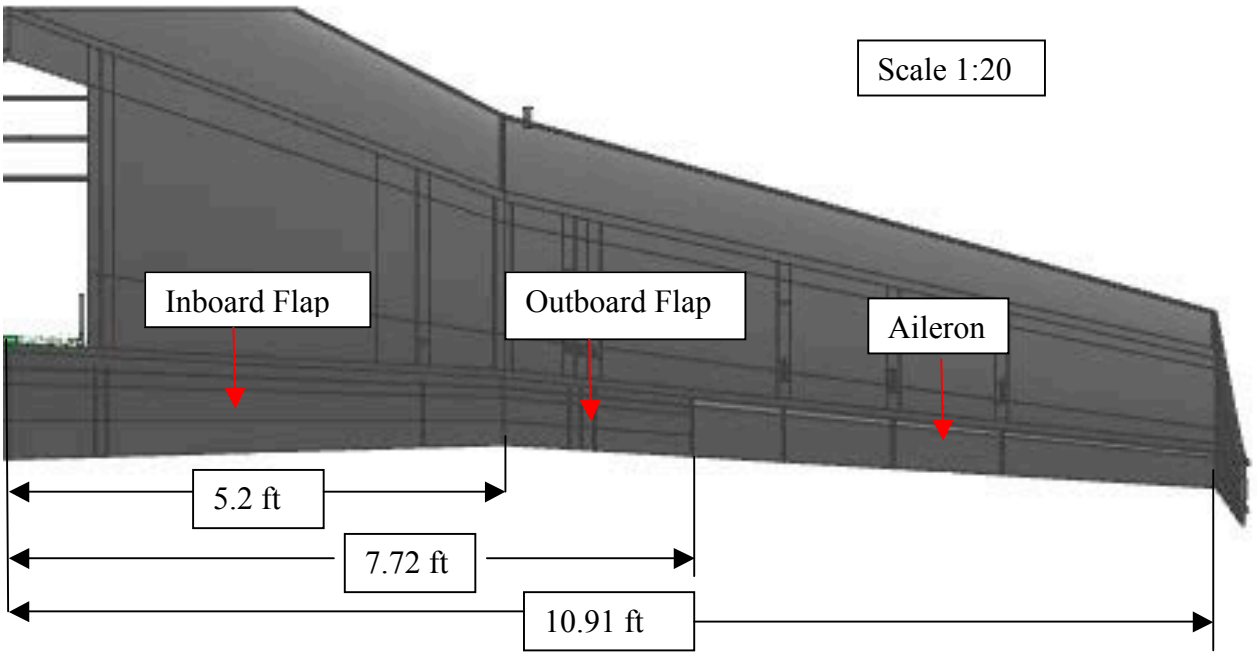

Figure 3-9: Aileron and Flap Dimensions

Because the wing is cranked, the flaps will be divided into two separate flaps per wing half. Shown in the table below one can see the ailerons geometric characteristics.

Table 3-6: Flap and Aileron Geometric Characteristics

Parameter	Flap	Aileron
$\frac{c_a}{c}, \frac{c_f}{c}$	.2	.2
η_o	0%	70%
η_i	70%	99%
t/c	8%	10%
δ_f	42 degrees	

Due to airfoil selection flaps are only required on landing.

Shown in the following figure one can see the wingtip airfoil with the aileron hinge. To prevent buffeting, which will be explained future in the report; the aileron hinges must not be aerodynamically balanced. Thus the following hinge design is used.

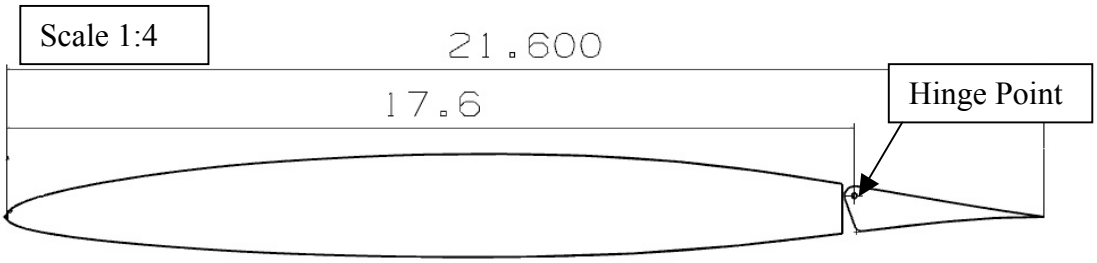

Figure 3-10: Wingtip Airfoil with Aileron Hinge

Shown in the following figure one can see the flap hinge, taken from the span wise location of wing crank, notice the split flap design.

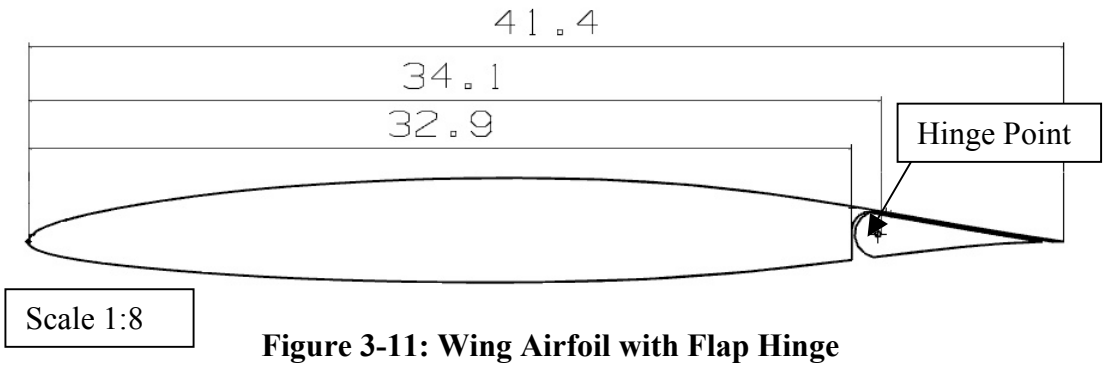

Figure 3-11: Wing Airfoil with Flap Hinge

3.3.3 Horizontal Tail and Elevator Sizing

Using the volume coefficient method, as presented in Reference 12 (pgs. 190-205), the horizontal tail is sized. Shown in the figure one can see the plan form of the horizontal tail.

Denoted by the purple outline one is able to see the elevator geometry, as well as the elevator hinge line, located at 1/3 of elevator chord, c_e. Shown in the following tables on the next page one can see the horizontal tail and elevator geometric characteristics.

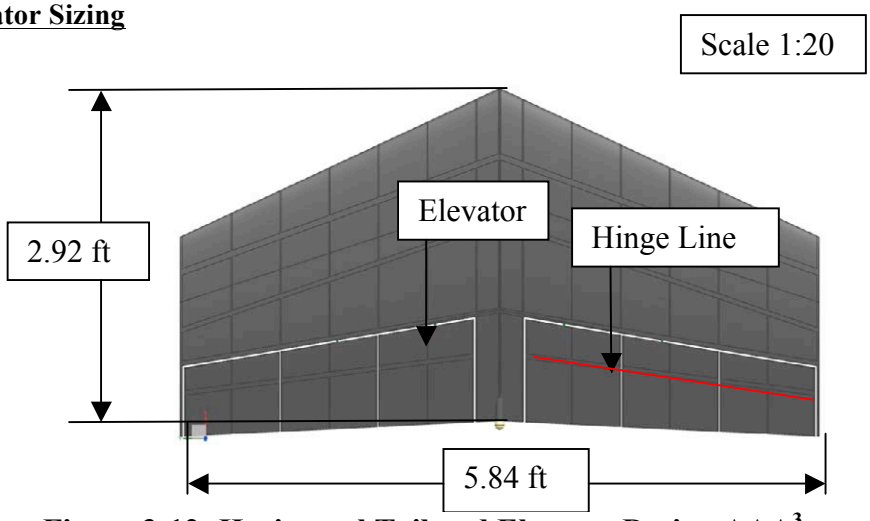

Figure 3-12: Horizontal Tail and Elevator Design AAA[3]

Table 3-7: Horizontal Tail Geometric Characteristics

Parameter	Value
Quarter chord sweep angle, $\Lambda_{c/4}$	20 degrees
Aspect Ratio, AR	2.51
Thickness ratio, t/c	10%
Taper ratio, λ	.6
Incidence, i_w	-0.30 degrees
Dihedral, Γ	1.5 degrees
Wash-out, ε_w	0 degrees
Area, S	13.7 ft^2
Airfoil	NACA 66-210

Table 3-8: Elevator Geometric Characteristics

Elevator	
V_h	.818 ft^3
S_e/S_h	0.381
S_e	5.31 ft^2
b_e	3.53 ft
η_{ie}	8 %
η_{oe}	95 %
c_{er}	1.27 ft
c_{et}	0.81 ft

3.3.4 Vertical Tail and Rudder Sizing

Much like the horizontal tail, the vertical tail was sized using the volume coefficient method, as presented in Reference 12 (pgs. 190-205). Shown in the following figure one can see the vertical tail and rudder plan form.

Denoted by the red outline one is able to see the rudder hinge line, located at 1/3 of rudder chord, c_r. Shown in the tables below one can see the vertical tail and rudder geometric characteristics.

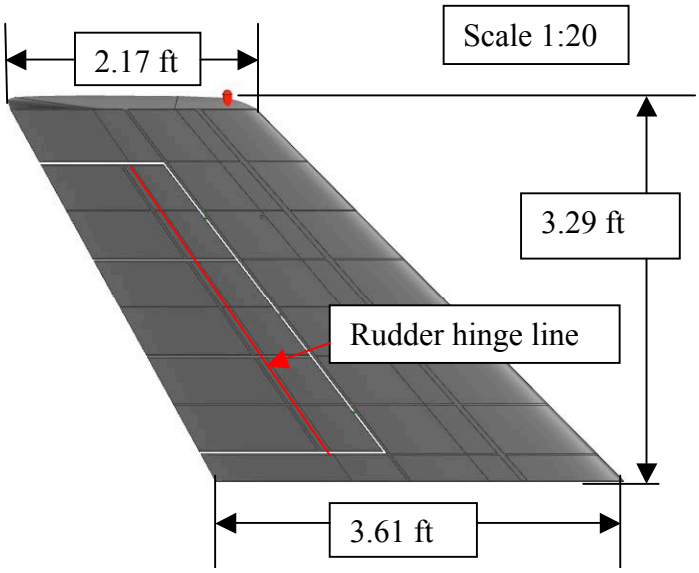

Figure 3-13: Vertical Tail and Rudder Design

Table 3-9: Vertical Tail Geometric Characteristics

Quarter chord sweep angle, $\Lambda_{c/4}$	40 degrees
Aspect Ratio, AR	1.14
Thickness ratio, t/c	11%
Taper ratio, λ	.6
Incidence, i_w	0 degrees
Dihedral, Γ	90 degrees
Area, S	9.5 ft^2
Airfoil	NACA SC0011

Table 3-10: Rudder Geometric Characteristics

Rudder	
V_v	.0921 ft^3
S_r/S_v	0.36
S_r	3.42 ft^2
b_r	2.53 ft
η_{ir}	8%
η_{or}	85%
c_r/c_v	30.6 %
c_{rr}	1.62 ft
c_{rt}	1.08 ft

3.4 Class I Aerodynamics

This section documents the Class I stall characteristics, drag polars and the L/D analysis using methods outlined in Reference 12 (Pgs. 281-294)

3.4.1 Stall

Using AAA[3] the following stall speeds were calculated.

Table 3-11: Stall Speeds

Takeoff	Race	Landing
138 knots	138 knots	109 knots

3.4.2 Drag Polar Analysis

Shown in the figure below one can see the perimeter plot that is generated from the previous figure.

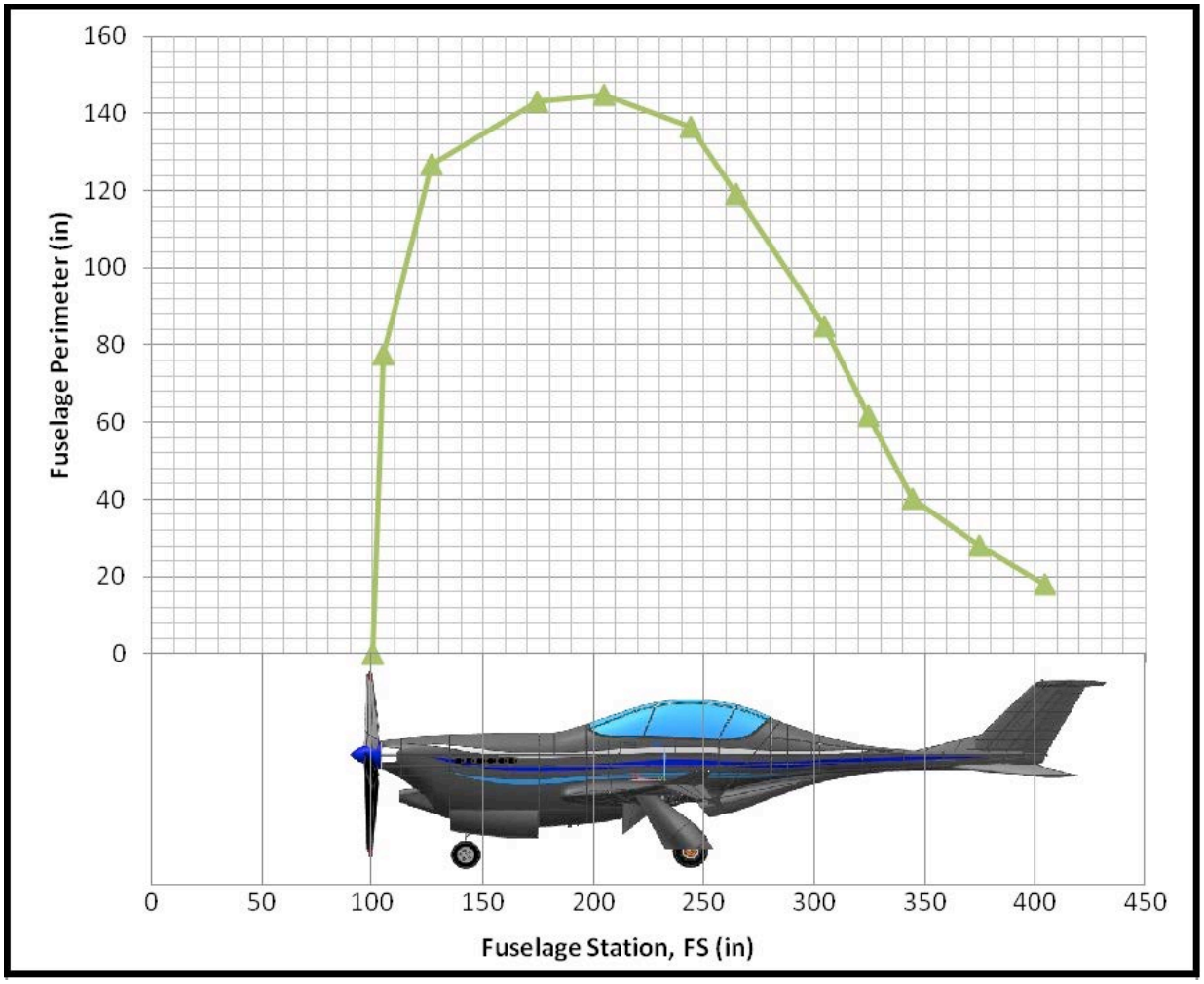

Figure 3-14: Fuselage Perimeter Plot

The wetted area for each component was measured using a CAD program, NX[2]. The wetted areas for each component are the following;

Table 3-12: Component Wetted Area

Item	Fuselage	Wing	Wing Fences	Horizontal Tail	Vertical Tail	Ventral Stakes	Dorsal Strakes	Total
Wetted Area, S ($ft^{2)}$	205	148	8.47	28.1	20.2	7.65	4.19	425

The addition increment to drag due to flap and landing gear were determined using Table 3.6 of Reference 14 (pgs. 127). Shown in the following table, one can see the incremental effects to C_{Do} due to flaps and landing gear.

Table 3-13: Drag Increments

	ΔC_{Do}	e
Race (clean)	0	0.85
Transonic Effects	.0004	No effect
Landing Gear	0.015	No effect
Takeoff Flaps	0	0.85
Landing Flaps	0.055	0.75

The induced drag of the Atlas RX is reduced by the wing fences; however, gives an equivalent aspect ratio of 110%. The drag polars including transonic compressibility effects can be seen in the table below.

Table 3-14: Atlas RX Drag Polars

	$C_{D_{race}} = C_{D_o} + \frac{C_L^2}{\pi A(1.1)e}$
Race (clean)	$C_{D_{race}} = 0.0127 + 0.0567C_L^2$
Takeoff Flaps	$C_{D_{TO}} = 0.0277 + 0.0567C_L^2$
Landing Flaps	$C_{D_{Land}} = 0.0827 + .0643C_L^2$

Shown in the figure below one can see the drag polar plots for race, takeoff and landing.

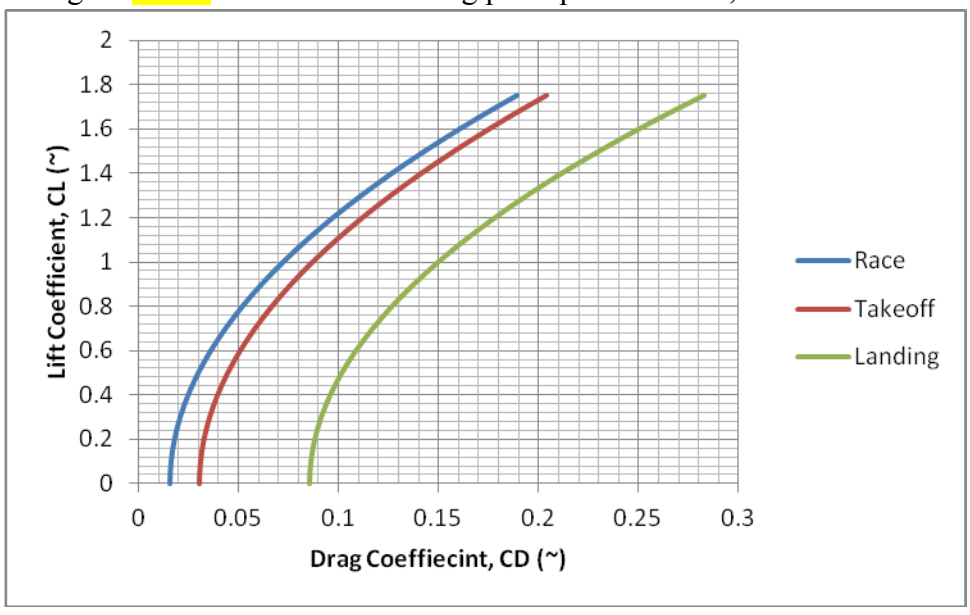

Figure 3-15: Drag Polar Plots

3.4.3 Analysis of Critcal L/D Results

Shown in the table below one can see calculated L/D ratios.

Table 3-15: Class I Lift-to-Drag Ratios

	L/D
Race	13.7
Takeoff	12.4
Landing	6.61

The initial lift to drag ratio used for preliminary design was 10. From the initial weight sensitivities presented previously, the increase in L/D would have the following effect:

$$\Delta W_{TO} = \Delta\left(\frac{L}{D}\right)\frac{\delta W_{TO}}{\delta \frac{L}{D}} \qquad \text{eqn. 3.1}$$

This results in a 0.798% increase in weight from the original takeoff weight. According to Reference 15, if the weight change is less than 5%, resizing of the airplane is not necessary.

3.5 Class II Landing Gear

From the calculated aft center of gravity, which will be discussed later in the report, the landing gear disposition is found. Shown in the figures below one can see the relative deposition of the landing gear, as well lateral and longitudinal tip-over criteria.

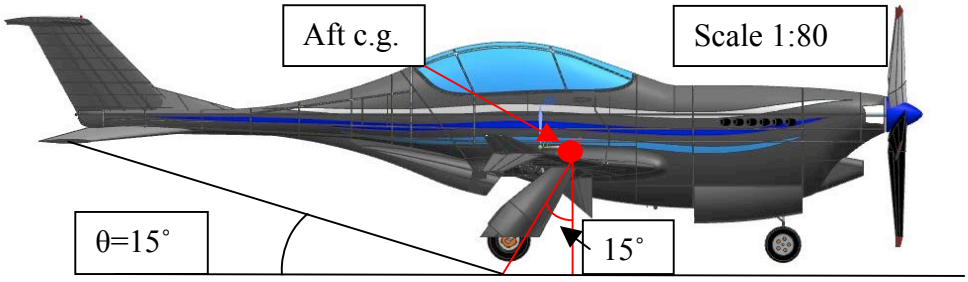

Figure 3-16: Lateral Tip-Over and Ground Clearance Criteria

Figure 3-17: Lateral Ground Clearance Criteria

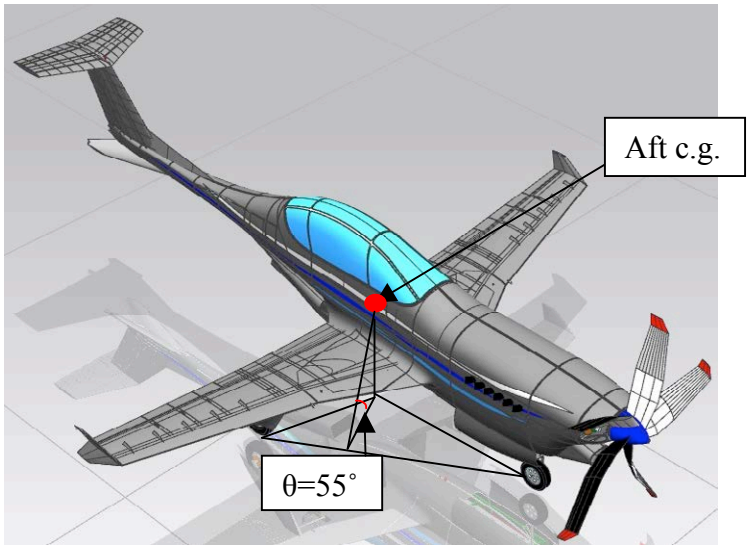

Figure 3-18: Longitudinal Tip-Over Criteria

When sizing the struts and tires for the Atlas RX methods described in Reference 16 (Pgs. 3-55) were used. The landing gear for the Atlas RX is a retractable tricycle configuration, which includes;

- Wheels
- Struts
- Braces
- Oleo shocks
- Brakes

The tires of the Atlas RX are sized according to Type I surfaces. The tire pressure and diameters were found using Reference 16. Type VII tires will be used for the Atlas RX for the following reasons;

- Higher pressure for high landing and takeoff speeds
- Low profile to be stored with in wing
- High load capacity (Ref. 16 Pgs 21)

Shown in the table below one can see the geometric characteristics of the landing gear.

Table 3-16: Landing Gear Sizing

	Main	**Nose**
Strut Diameter, d_s	0.172 ft	0.137 ft
Strut Stoke, s_s	0.494 ft	0.23 ft
Rake	-25˚	-3˚
D_t x b_t	18” x 4.4”	16” x 4.4”
Tire Pressure	185 psi	55 psi
Max Static Load	3,270 lbs	967 lbs
Min Static Load	~	645 lbs
Dynamic Load	~	1350 lbs

According to tire data provided by Reference 16 (Tables 2.5-2.16); these loads are well within the allowable loading range for Type VII tires.

The nose wheel-strut interface of the Atlas RX had been designed to be both statically and dynamically stable by placing the wheel axel and tire-ground contact point aft of the wheel swivel axis. The interface was made dynamically stable for the following reasons;

- Runway-to-tire friction will cause the wheel to rotate to correct position
- Both differential braking as well electrical pistons attached to the nose strut can be used for ground steering

The nose gear strut has a negative rake as it is mounted to the lower side of the engine integration mount. The main gear much like the nose gear strut has negative rake, as well as positive trail, making the main gear both dynamically and statically stable.

4 Three-View General Arrangement and Salient Characteristics

In the following chapter one will present the general arrangement of the aircraft and components.

Figure 4-1: Atlas Rx Isometric View

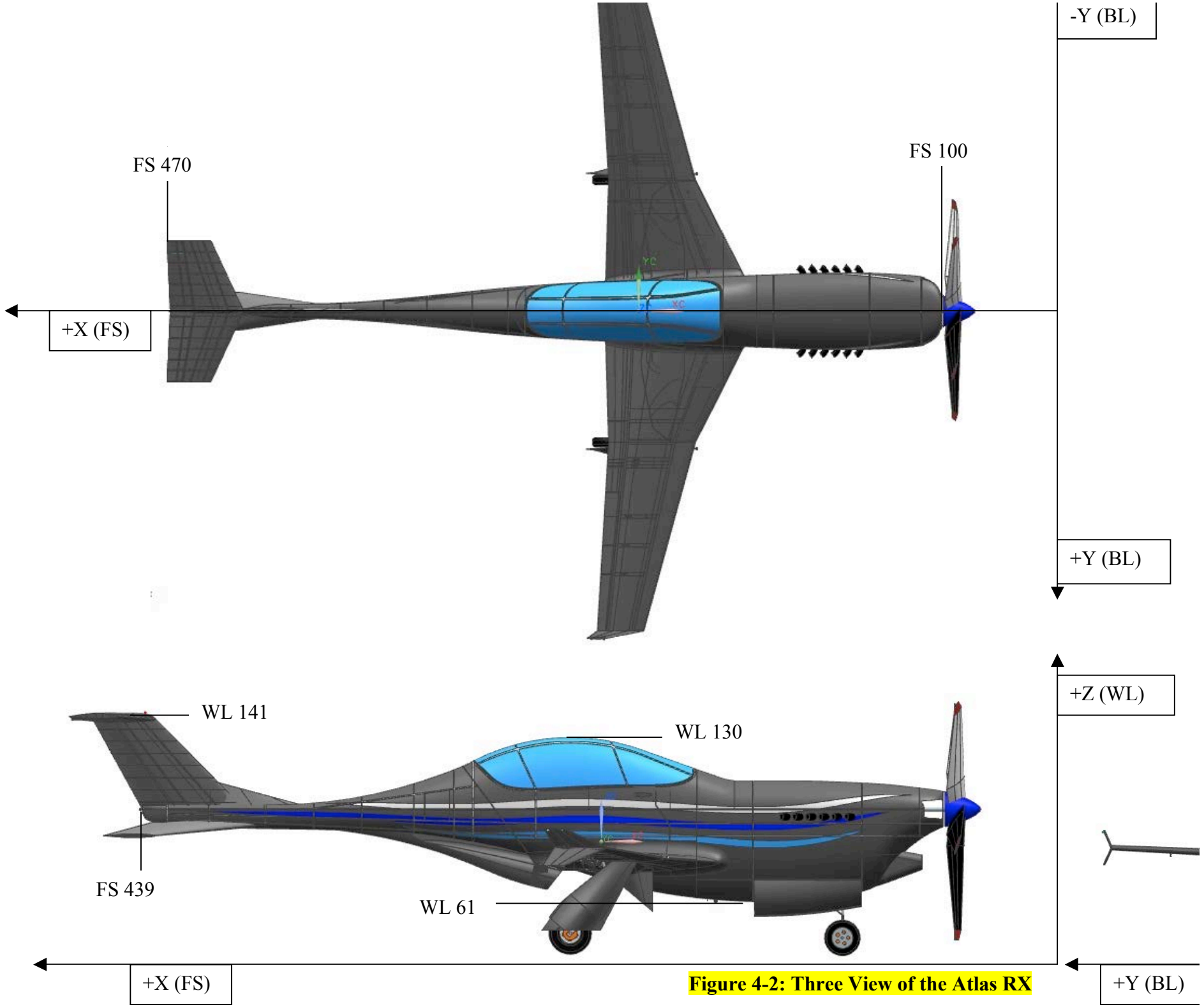

Figure 4-2: Three View of the Atlas RX

4.1 Salient Characteristics

Table 4-1: Salient Characteristics of the Atlas RX

	Wing	Horizontal Tail	Vertical Tail
Area	81 ft^2	13.7 ft^2	9.5 ft^2
Span	22.1 ft	5.84 ft	3.29 ft
MGC	3.99 ft	1.34 ft	2.95 ft
MGC L.E.: FS	9.5 ft	28.4ft	34.4 ft
Aspect Ratio	6	2.51	1.14
Sweep Angle, (c/4)	15.5 deg	20 deg	40.1 deg
Taper Ratio	0.32	0.60	0.60
Thickness Ratio	0.10	0.10	0.11
Airfoil	NACA 66-210	NACA 66-210	NACA SC0011
Dihedral Angle	2.8 deg	2 deg	90 Deg
Incidence Angle	2 deg	-0.30 deg	0 deg
Aileron Chord Ratio	.2	Elevator Chord	Rudder Chord
Aileron Span Ratio	.7-.99	Ratio: .0209-.251	Ratio: .0273-.23
Flap Chord Ratio	.2	~	~
Flap Span Ratio	0-.7	~	~
	Fuselage	Cockpit	Overall
Length	28.3 ft	8.33 ft	32.1 ft
Maximum Height	5.75 ft	4.5 ft	8.58 ft
Max Width	3.04 ft	2.52 ft	22.7 ft

5 Inboard Profile

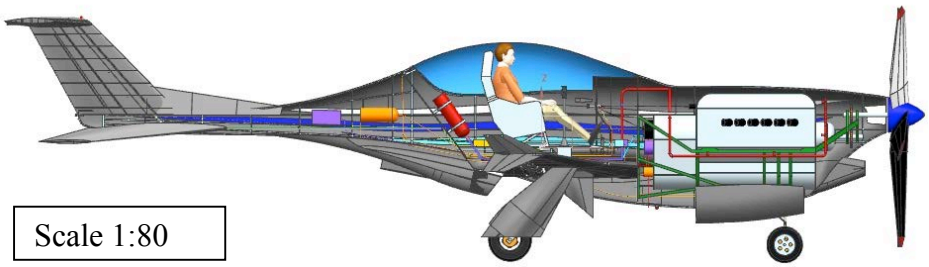

Figure 5-1: Cut-Away View

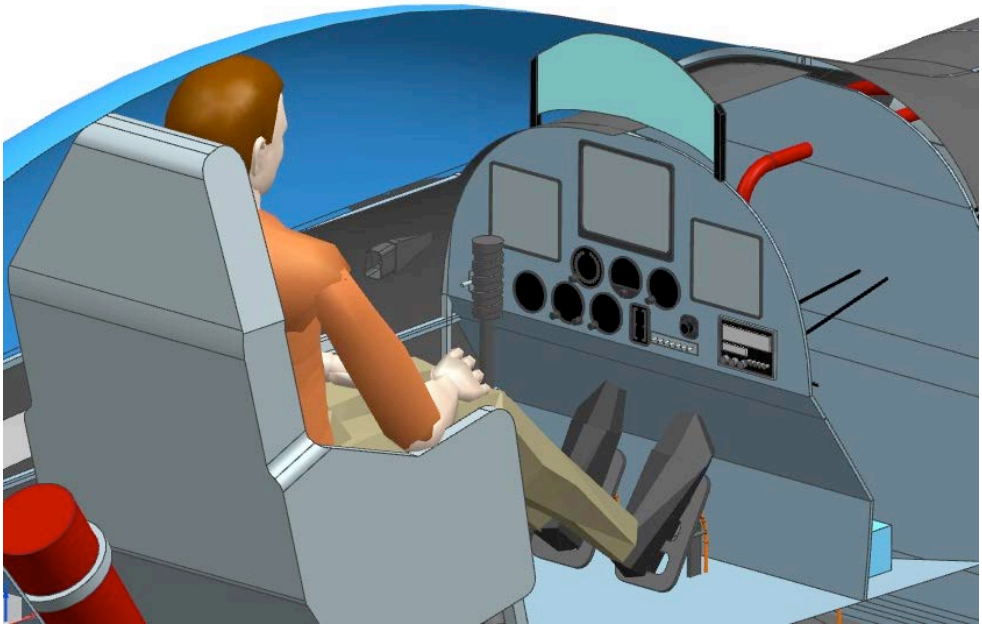

Figure 5-2: Cockpit Detail View

Shown in the figure below, one can see the engine bay doors open for engine access and maintenance.

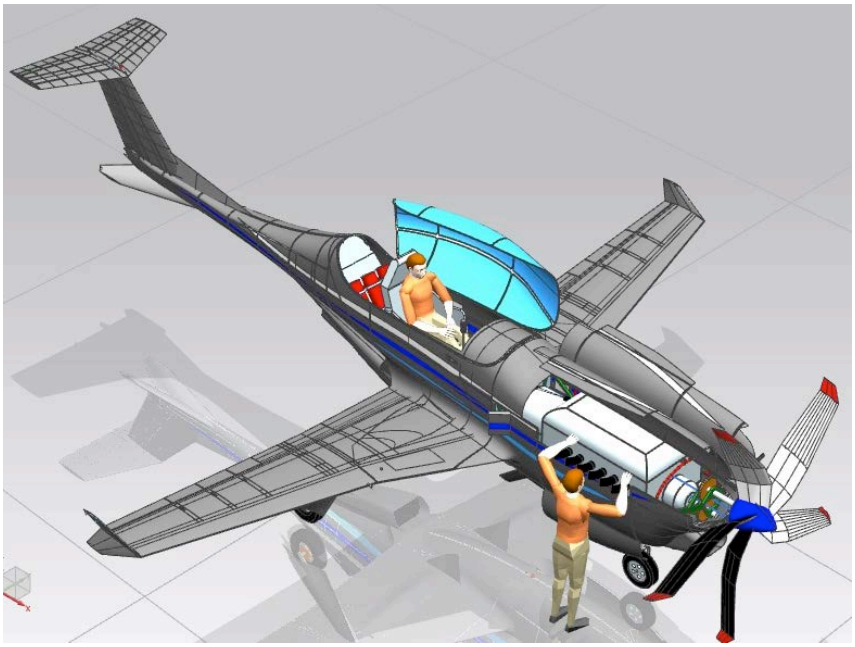

Figure 5-3: Engine Doors Open

Shown in the following figure one can see the engine doors and propeller off the aircraft to allow access for engine replacement. Note the tail stand to prevent the airplane from falling on its tail as the engine is removed.

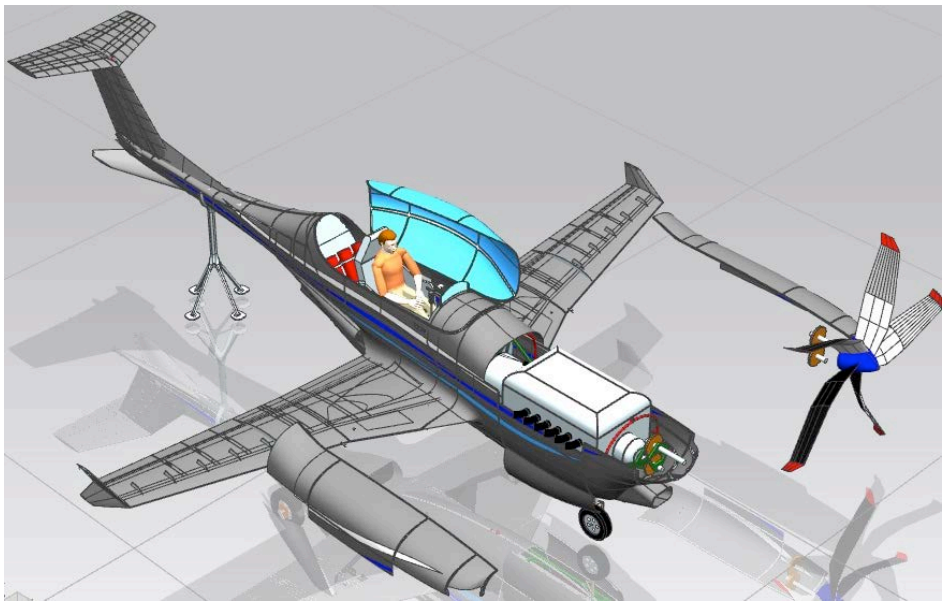

Figure 5-4: Engine Doors Off for Engine Removal

Engine hoist is still to come

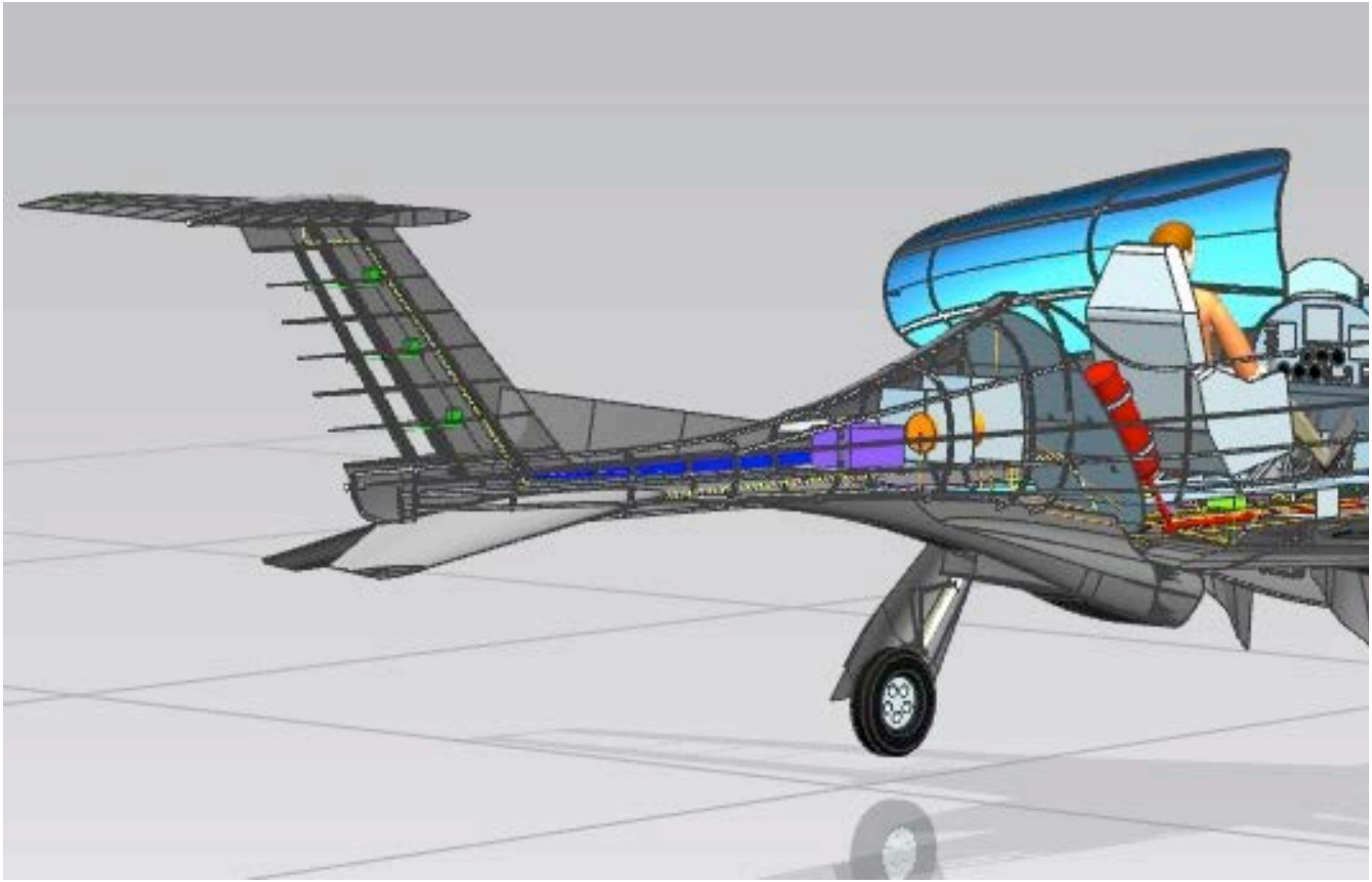

Figure 5-5: Detail View

\

6 Weight Break Down and C.G. Excursion Diagrams

The following section presents the component weight breakdown and c.g. excursion diagrams.

Table 6-1: Weight Specifications

W_E (lbs)	W_{TO} (lbs)	W_{crew} (lbs)	W_F (lbs)	M_{FF}	$(W/S)_{TO}$ (lb/ft^2)	$(W/P)_{TO}$ (lbs/hp)	P (HP)	S (ft^2)
4500	5010	200	1250	.791	62.3	3.34	1500	81

Table 6-2: Component Weight Breakdown

#	Component	Weight (lbs)	Xcg, FS (in)	Ycg, BL (in)	Zcg, WL (in)
1	Wing Group	350	230	0	79.0
2	Horizontal Tail	250	447	0	143
3	Vertical Tail	250	422	0	117
4	Ventricle Strakes	100	411	0	97.4
5	Fuselage Group	715	313	0	100
6	Nose Gear	65	142	0	56.0
7	Main Gear	100	252	0	65.0
8	Engine	1640	155	0	89.2
9	Propeller	150	95	0	100
10	Electical	60	335	0	97.2
11	Avionics	20	221	0	97.2
12	Funishings	200	266	0	107
13	Hydraulic	45	306	0	98.8
14	Flight Sytem 1	15	270	0	87.6
15	Flight Sytem 2	15	247	0	85.8
16	Flight Sytem 3	15	221	0	88.5
17	Fire Extinguisher	65	211	0	99.3
18	Air-Pneumatic	40	221	0	76.3
19	Engine Starter	20	200	0	93.1
20	Electric Generator	20	200	0	85.8
21	Air Pump	30	200	0	93.1
22	Hydraulic Pump x 2	35	200	0	76.3
23	Radiator	300	281	0	77.3
24	Fuel	310	215	0	79.0
25	Trapped Fuel and Oil	15.5	155	0	89.2
26	Crew	184.5	256	0	107

Table 6-3: Center of Gravity Location

	Aft	Forward
X_{cg}	244 inches	242 inches
Z_{cg}	94.8 inches	94.5 inches

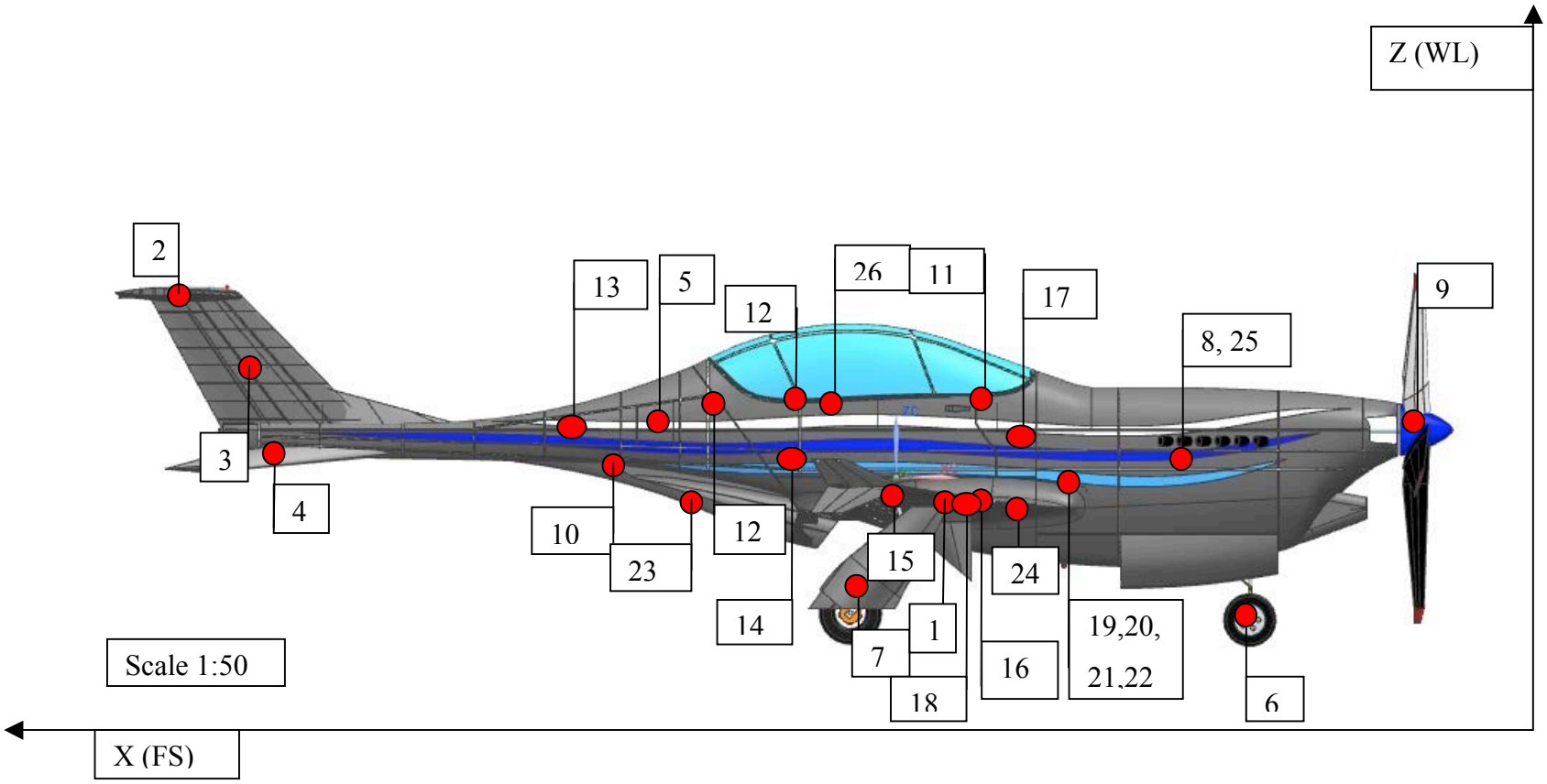

Figure 6-1: Component CG Location Presented on the Aircraft

Refer to Table 6-2: Component Weight Breakdown for numbering system.

Shown in the figure below one can see the disposition of the aft most center of gravity.

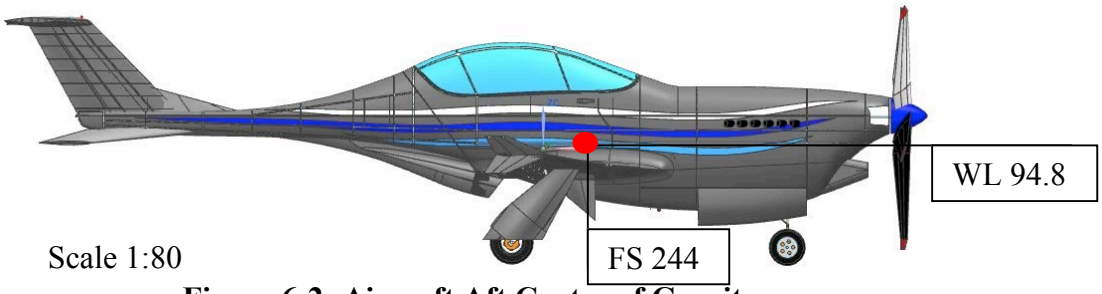

Figure 6-2: Aircraft Aft Center of Gravity

Shown in the figure below on can see the plotted c.g. excursion diagram.

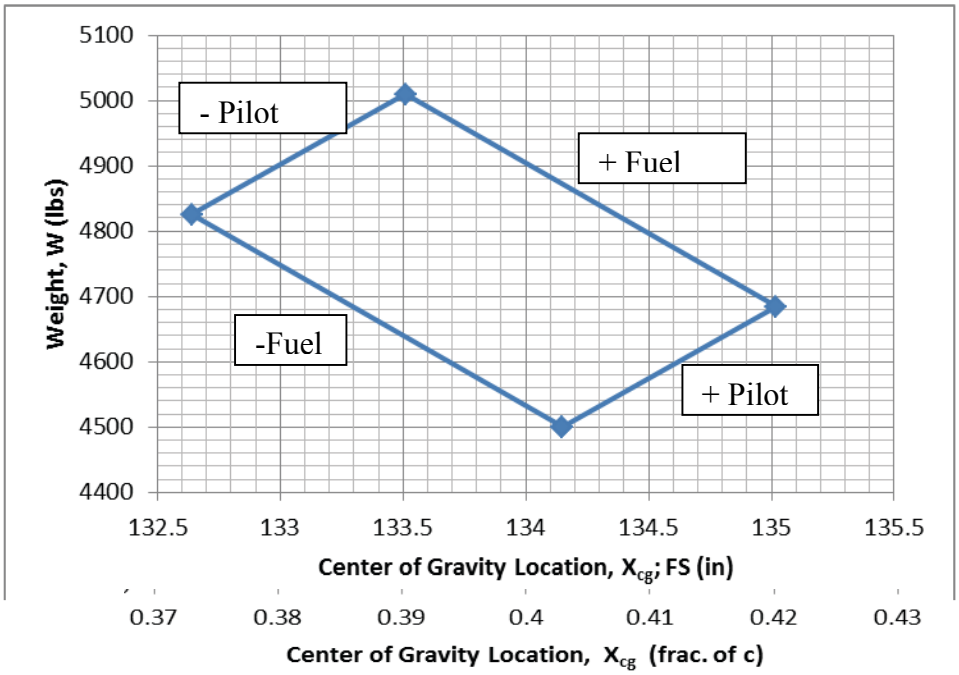

Figure 6-3: Center of Gravity Excursion

The calculated cg shift within the excursion plot is -1.34% of mgc, or 0.64 inches. As the majority is due to when the pilot boards the aircraft, it can be assumed that as the Atlas RX races around the track the center of gravity shift will not change. This is proven as the calculated value of center of gravity shift is only 0.03% of mgc when fuel is added or burned.

Shown in the figure below one can see the c.g. excursion presented on the aircraft.

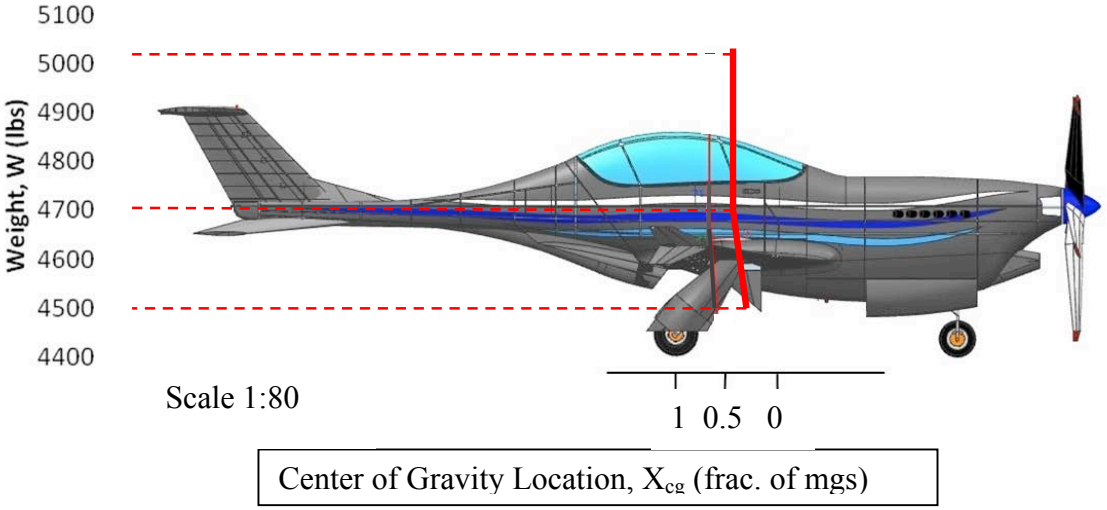

Figure 6-4: Center of Gravity Excursion Presented on the Aircraft

Shown in the figure below one can see the moments of inertia generated by AAA[3]

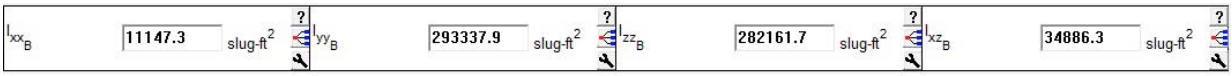

Figure 6-5: Moments of Inertia AAA[3]

7 Class II Drag Build-Ups & Drag Polars

Shown in the figure below one can see the drag polar build up generated by AAA[3]

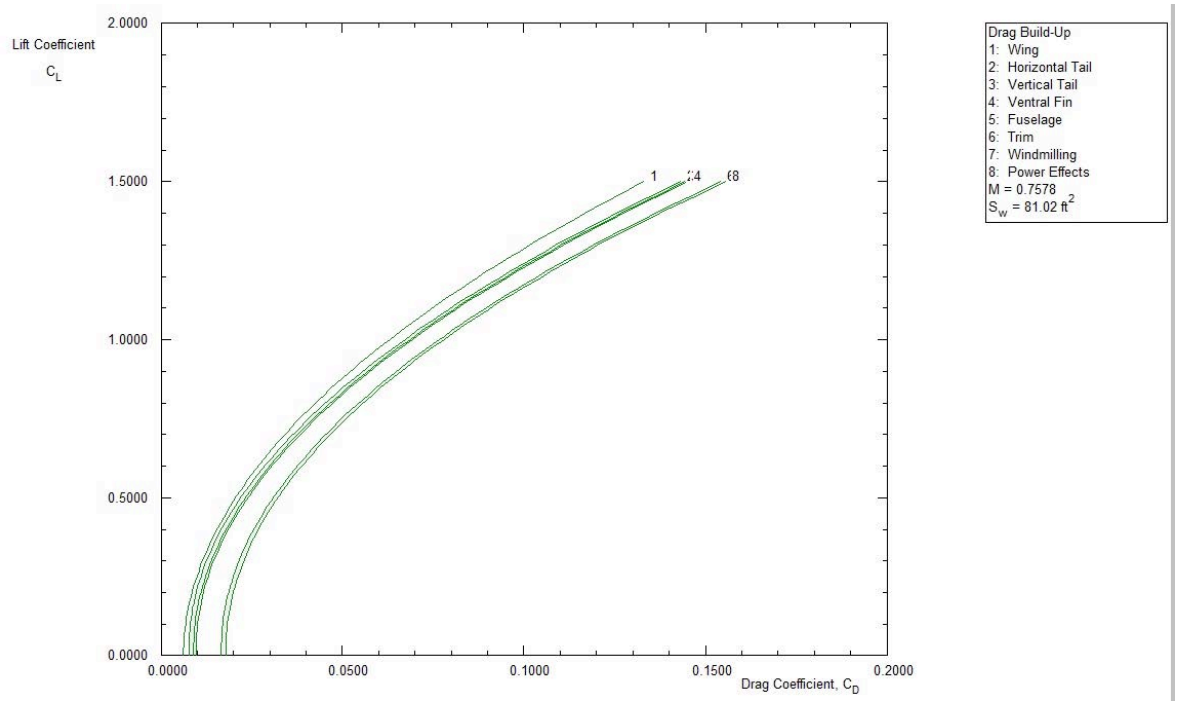

Figure 7-1: Class II Drag Build-Ups AAA[3]

Shown in the figure below one can see the Class II drag polar generated by AAA[3].

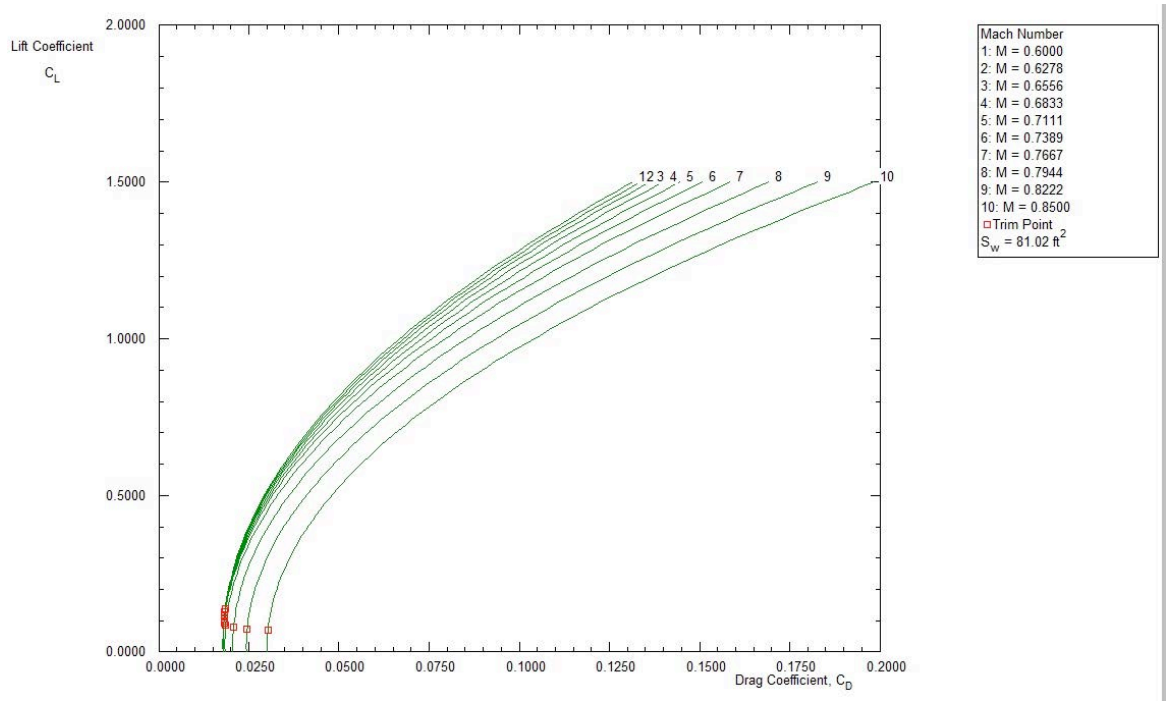

Figure 7-2: Class II Drag Polars AAA[3]

Takes into account compressibility

8 Class II Propulsion Performance

This section documents the verification of propulsion performance to confirm the Atlas RX meets all RFP requirements.

8.1 Power Extraction

When computing the horsepower required to run the systems of the aircraft, methods outline in Reference 15 (pgs. 139-212) were used. Using the equations presented below, the extracted power is calculated.

$$P_{extr} = P_{el} + P_{mech}$$ eqn. 7.1

Reference 15, Equation 6.1

Electrical extracted power

$$P_{el} = \frac{.00134(VA_{plp})}{\eta_{gen}}$$ eqn. 7.2

Reference 15, Equation 6.2

$\eta_{gen} = 0.9$

VA_{plp} is found to be 8910 VA from the required volts and amps needed to run the navigation lights, Reference 17, and flight control actuators, Reference 17, resulting in P_{el}=11.9 hp.

Mechanical extracted power

$$P_{mech} = P_{fp} + P_{hydr} + P_{other}$$ eqn. 7.3

Reference 15, Equation 6.3

Mechanical power required to drive the fuel pump

$$P_{fp} = \frac{0.00014\left(c_p\right)SHP}{\eta_{fp}}$$ eqn. 7.4

Reference 15, Equation 6.4

c_p=.9

$\eta_{fp} = 0.65$

SHP=1500 hp

P_{fp}=.29 hp

Mechanical power required to drive the hydraulic pump

$$P_{hydr} = \frac{0.0006\left(\Delta p_{hydr}\right)\left(\dot{V}_{hydr}\right)}{\eta_{hydr}}$$ eqn. 7.5

Reference 15, Equation 6.5

$\eta_{hydr} = .75$

Δp_{hydr}=1000 lb/in^2

$\dot{V}_{hydr}$=2.5gal/min

P_{hydr} =2.00 hp

P_{mech}=2.29 hp

P_{extr}=14.1 hp

8.2 Takeoff Distance

Reno's Stead Field have a runway length of 7600 ft and 9080 ft, to ensure the aircraft is able to take off with the minimum distance methods described in Reference 19 (pgs. 117-123) were used along with AAA[3] adhering to military specifications and Class IV high maneuverability aircraft. Shown in the figure below one can see the takeoff distance diagram.

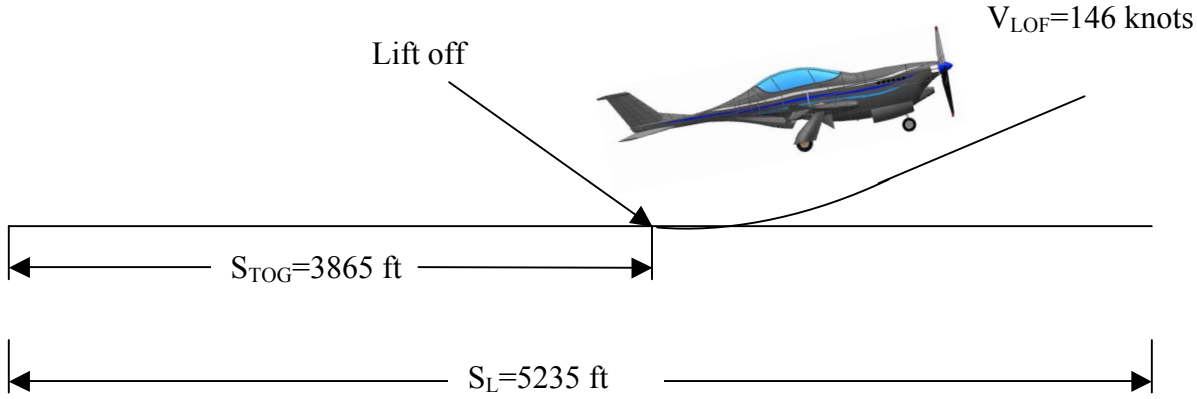

Figure 8-1: Military Takeoff Distance

8.3 Cruise Performance

The RFP requires that the aircraft must be competitive in the unlimited category of the Reno Air Races as well as be able to perform a 500nmi ferry mission. For this to happen the Atlas RX must be able to fly faster than 500 mph while in the race and have a low enough specific fuel consumption to be able to make the entire 500nmi mission. With a propeller efficiency of 0.75, L/D of 12.4, specific fuel consumption of .37 for ferry and .9 for race and 310 lbs of fuel, the Breguet range equation, shown in eqn. 7.1, was used to find that the Atlas RX is capable of a 523nmi ferry mission.

$$R(nmi) = 325.9\left(\frac{nmi - lbf}{hp - hr}\right)\left(\frac{\eta_p}{c_p\left(\frac{lbf}{hp - hr}\right)}\right)\left(\frac{L}{D}\right)Ln\left(W_{initial}/W_{final}\right) \qquad \text{eqn. 7.1}$$

The reason for the specific fuel consumption being lower in the ferry mission compared to the race is due to the assumption that the engine will not be running at full power, nor will it be running on all engine cylinders.

Using methods described in Reference 19 (pgs. 117-123) were used along with AAA[3] the maximum cruise speed is calculated. Shown in the figure to the right, one can see the power vs. velocity plot AAA[3].

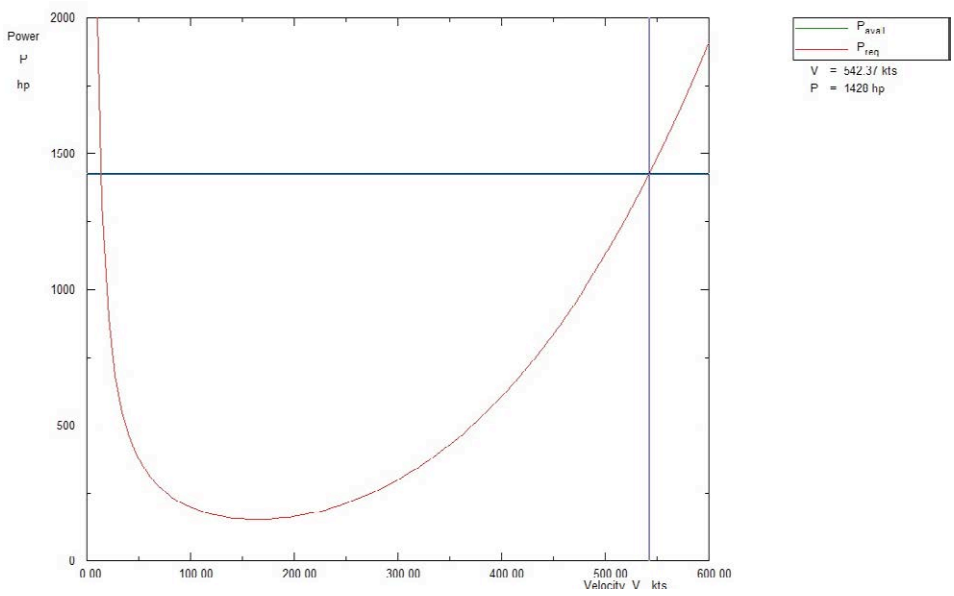

Figure 8-2: Maximum Cruise Speed AAA[3]

It is seen that the Atlas RX, in race configuration, will be able to fly 542 knots, or 625 mph, well faster than any current aircraft in the unlimited class of the Reno Air Race, or any class for that matter, even jets. Not only will the Atlas RX be competitive, it will break any and all currently standing records for Reno Air Races.

8.4 Critical Mach Number

Due to the capabilities of the Atlas RX, the concern for critical Mach number arose. Using AAA[3], the values for each major component of the aircraft were found. Shown in the following table one can see the calculated critical Mach numbers.

Table 8-1: Component Critical Mack Number

Wing	0.858
Horizontal Tail	0.912
Vertical Tail	0.907
Ventral Strake	1.06

8.5 Maneuvering

Methods described in Reference 19 (pgs. 150-158) were used along with AAA[3] to calculate the maneuverability of the aircraft. Shown in the equations below one can see the turn rate, turn radius and g loading for sustained level turn.

$$\phi_{turn} = \tan^{-1}\left(\sqrt{n_{turn}^2 - 1}\right) \qquad \text{eqn. 8.1}$$

$$n_{turn} = 8.65$$

$$R_{turn} = \frac{V_M^2}{g * \tan\left(\phi_{turn}\right)} \qquad \text{eqn. 8.2}$$

$$V_M^2 = 500 knots$$

$$R_{turn} = 9570\, ft$$

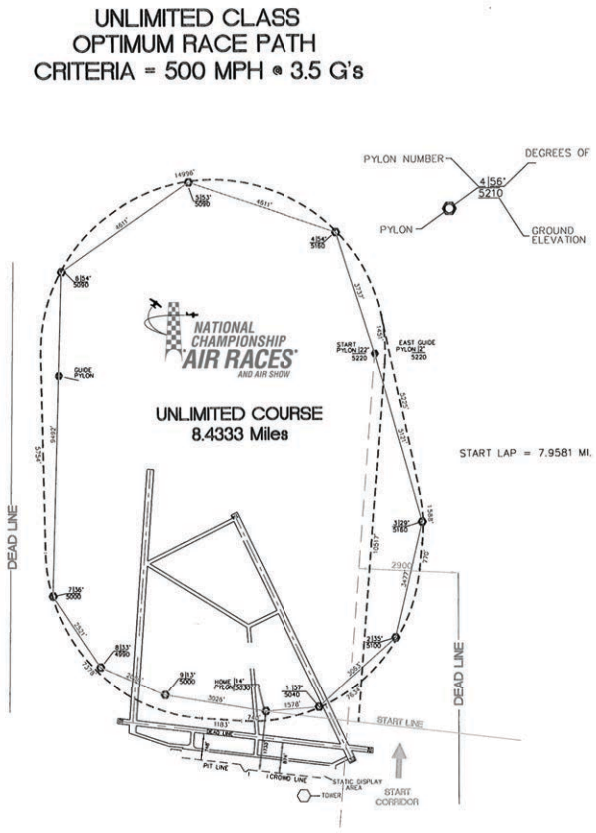

Figure 8-3: Reno Flight Track (ref. 20)

From this minimum turning radius; one is then able to plot a flight course. It is found that the Atlas RX has a lap time of 52.1 seconds and with a 6 lab course, the total race time is 5:12.6, beating the record lap time, set in 2003 Reference 21, by more than 45 seconds.

8.6 Landing Distance

To ensure the aircraft is able to land with the available distance, methods described in Reference 19 (pgs. 162-166) were used along with AAA[3]. Shown in the figure below one can see the landing distance diagram.

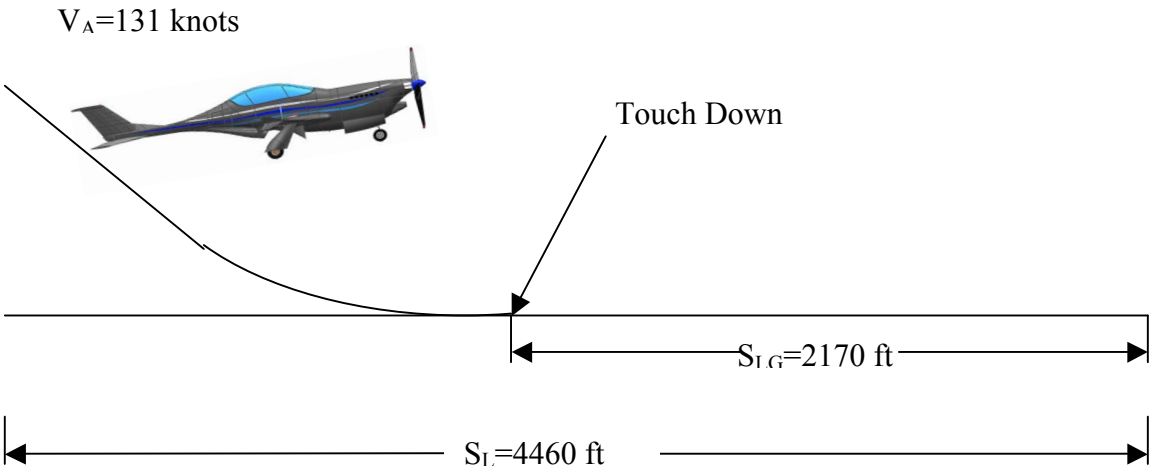

Figure 8-4: Military Landing Distance

One will note that the landing distance, S_L, is well below 7600 ft, which is the length of the runway at Stead Field.

9 Class I & II Stability and Control

9.1 Class I Stability and Control

In this section the author will present the Class I stability and control analysis using the step-by-step method in Reference 12 (Pgs. 259-280).

After preliminary sizing of the horizontal tail, using the volume coefficient method, it was determined that the Atlas RX would be controlled by an irreversible system, thus allowing the static margin to be 0. Upon the initial calculations of aerodynamic center location, $\bar{x}_{ac}$, positions of weight components were manipulated to match this value. Shown in the figure below one can see the longitudinal X-plot.

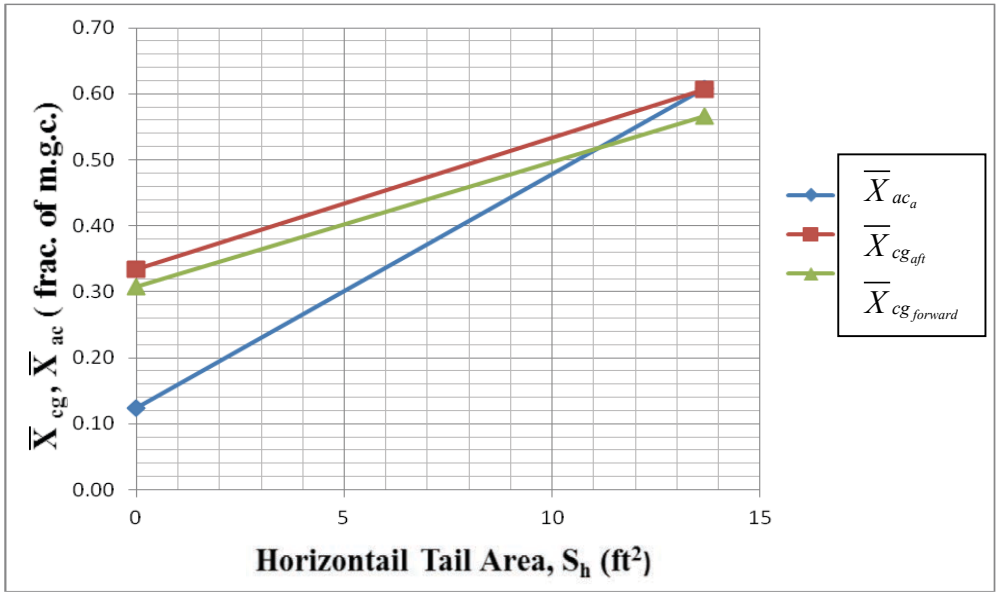

Figure 9-1: Longitudinal X-Plot

One will notice the matching points of $\bar{x}_{ac}$ and $\bar{x}_{cg,aft}$, converging at a horizontal tail area of 13.65 ft^2, thus proving a static margin to be 0.

When computing the directional stability for the Atlas RX a vertical tail area, S_V, was assumed to be 9.5 ft^2, the exact value found using the volume coefficient method. Shown in the figure below one can see the directional X-plot.

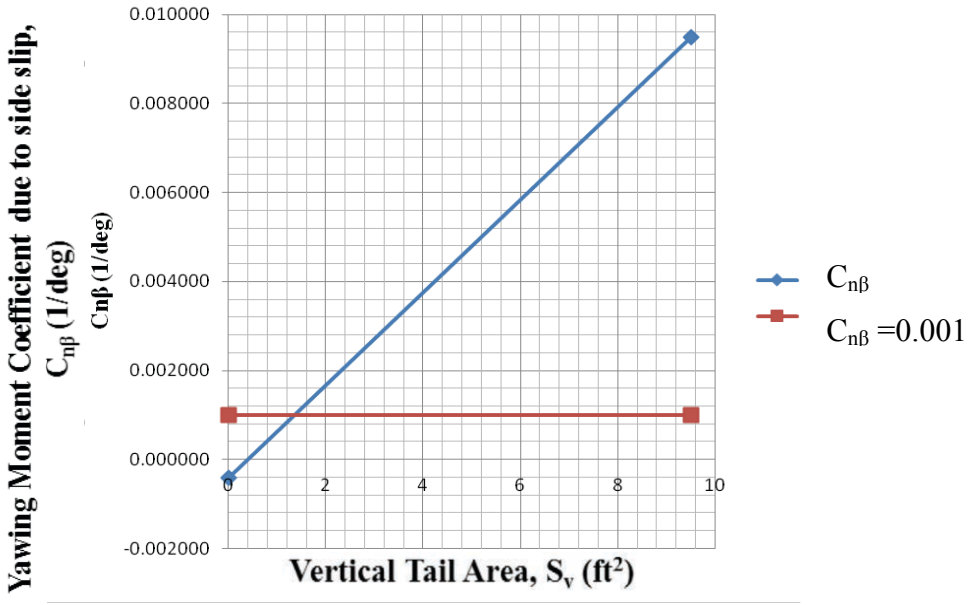

Figure 9-2: Directional X-Plot

Marked by the red line, the minimum vertical tail area for directional stability, a value of 9.5 ft^2 is sufficient for Atlas RX vertical tail area.

9.2 Class II Stability and Control

When calculating the Class II stability and control for the Atlas RX the step-by-step methods presented in Reference 19 (pgs. 5-175) were used in addition to AAA^3. From these calculations some of the final general arrangements of components were finalized to allow the Atlas RX perform to its highest degree.

9.2.1 Trim Diagram

Shown in the following figures one can the plotted trim diagram using AAA^3.

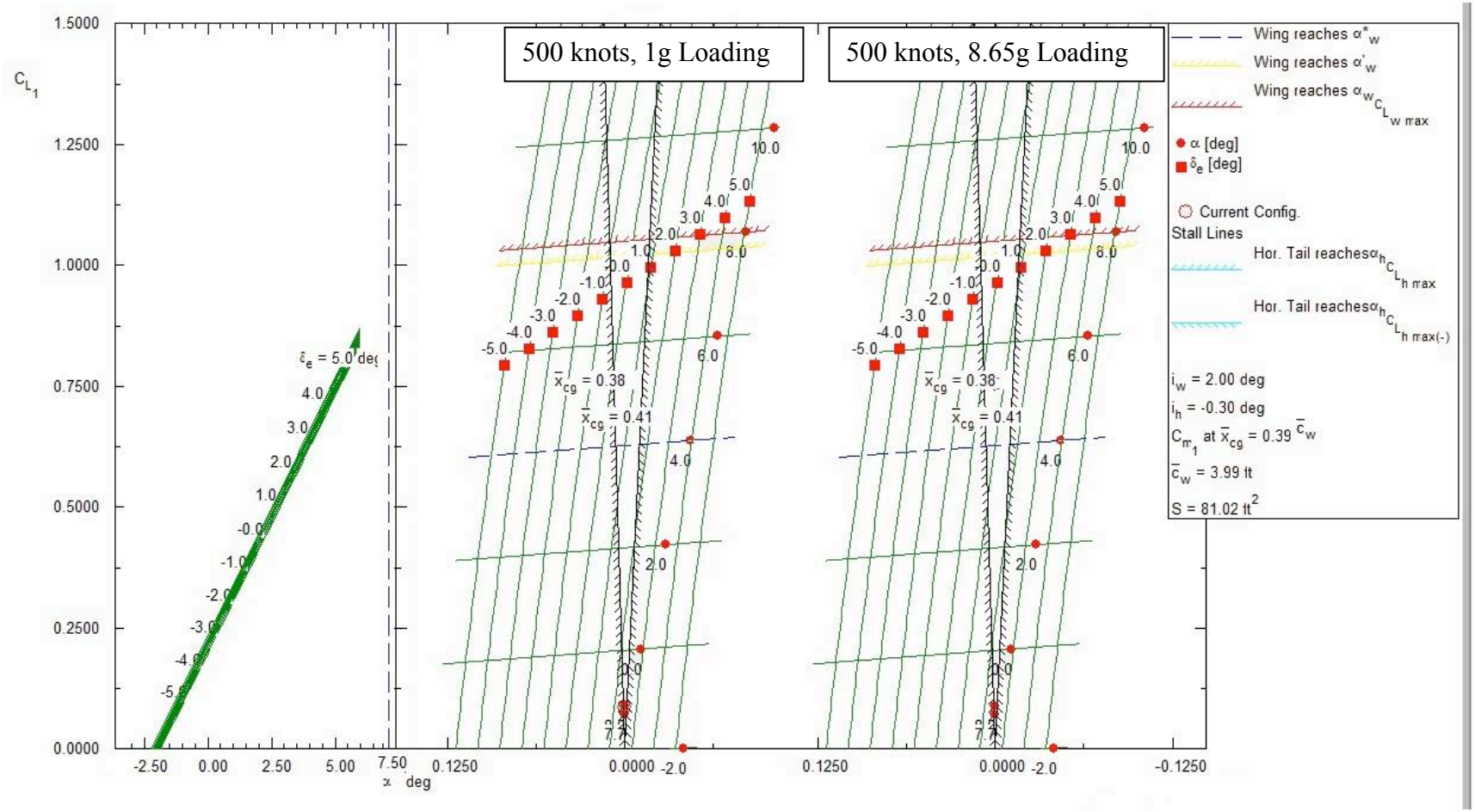

Figure 9-3: Class II Stability and Control Race Trim Diagram; 500 Knots, 1 g & 8.65g Loading AAA[3]

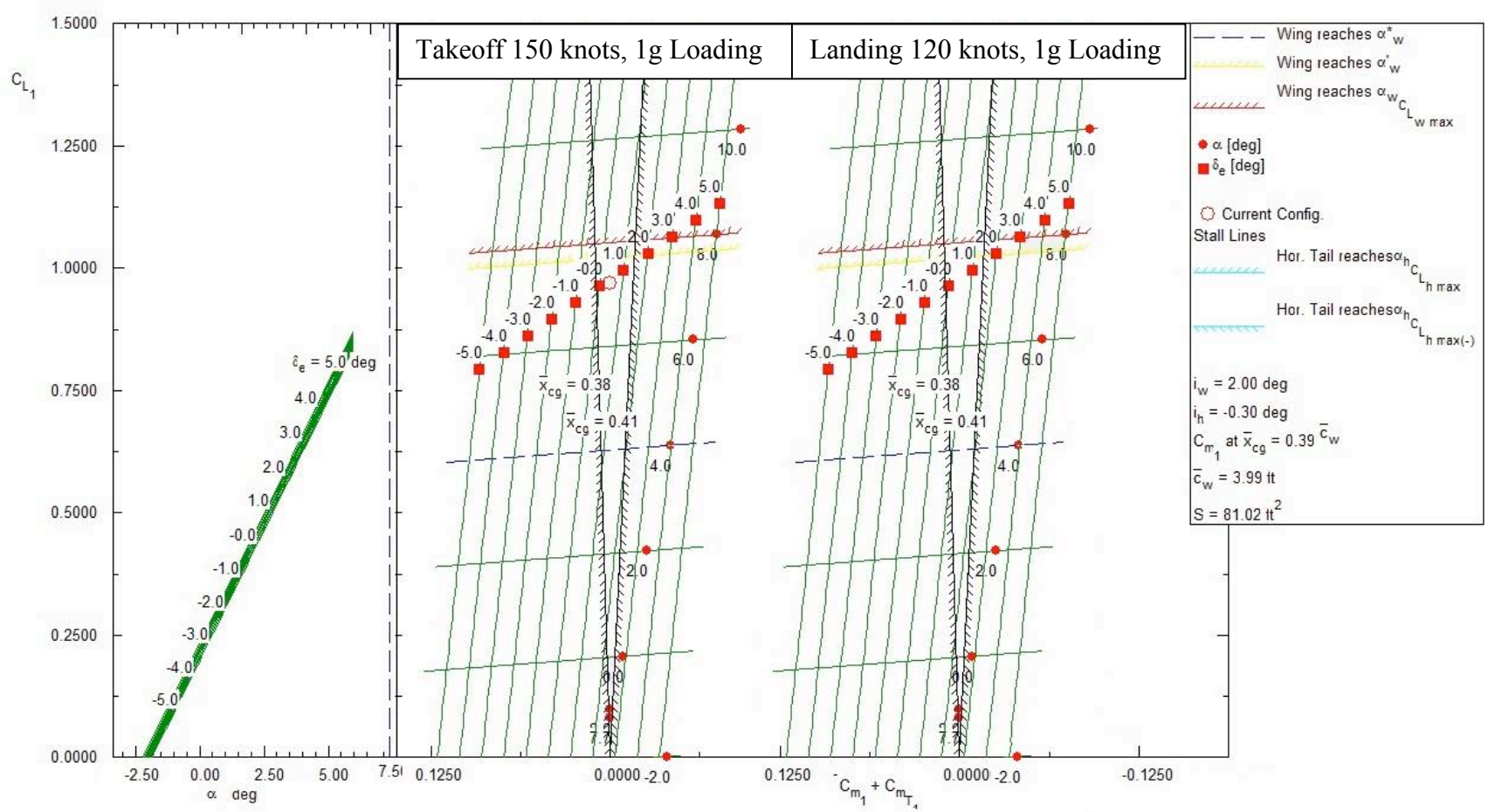

Figure 9-4: Class II Stability and Control Takeoff Trim Diagram; 150 Knots, 1 g Loading & Landing Trim Diagram; 120 Knots, 1 g Loading AAA[3]

Prior to finalizing the trim diagram, the incidence of the horizontal tail, i_h, was assumed to be 0. However; based on desired flying characteristics, i_h was found to be -0.30 degrees. Based on the flight conditions, it is apparent that the aircraft is highly susceptible to elevator deflection, δ_e, which remains apparent as the dynamic pressure on the elevator is rather high. Notice that the aircraft only needs 1 degree of elevator deflection to remain in the flight wind, denoted by the slashed black lines. Thus if one of the triple redundant elevator actuators were to malfunction the maximum deflection needed by the remaining elevator actuators would only by three degrees

It is realized that the Atlas RX will not need a stability augmentation systems with a feedback gain, as the static margin, SM, found from the trim diagrams is a positive value for each flight condition, which holds true from the Class I stability and control static margin. From the equation below the static margin for each flight condition is calculated.

$$\frac{\Delta C_m}{\Delta C_L} = \Delta SM \qquad \text{eqn. 9.1}$$

Table 9-1: Feedback Gain

	$\frac{\Delta C_m}{\Delta C_L}$
Race; 500 knots, 1 g	4.54 %
Race; 500 knots, 8.65 g	4.55%
Takeoff; 150 knots, 1 g	3.57%
Landing; 120 knots, 1 g	3.63%

From these numbers it is seen that the Atlas RX is inherently longitudinally stable. However; being that the values are rather low; the aircraft must be flown by pilot with the highest experience. This can be over looked as all Reno pilots are of the highest skill in their field.

9.2.2 Spiral, Dutch Roll and Phugoid

Shown in the table below, one can see the natural frequency, ω, and damping ratio, ξ, for spiral, dutch roll and phugoid. These values were found using AAA#.

Table 9-2: Spiral, Dutch Roll and Phugoid Natural Frequency and Damping Ratio

Short Period	
ω_{nSP}	3.87 rad/sec
ς_{SP}	.355
Phugoid	
$\omega_{n_{P\_long}}$	.198 rad/sec
$\varsigma_{P_{long}}$	.274
Dutch Roll	
ω_{n_D}	.4019 rad/sec
ς_D	-0.839

10 Structures

10.1 Fuselage Structure

The fuselage will be that of both full and semi monocoque structure made from composite materials, mostly carbon fiber and fiberglass. With the use of composite ring frames and paneled skins, the manufacturing process and assembly time will be greater than that of a fully monocoque structure, yet precision of manufacturing is of the highest degree. Preliminary sizing was performed as follows;

- Average skin thickness: 0.03”
- Firewall thickness: 0.188”
- Bulked thickness: 0.125”
- Ring frame thickness: 0.05”
- Stringer thickness: .04”

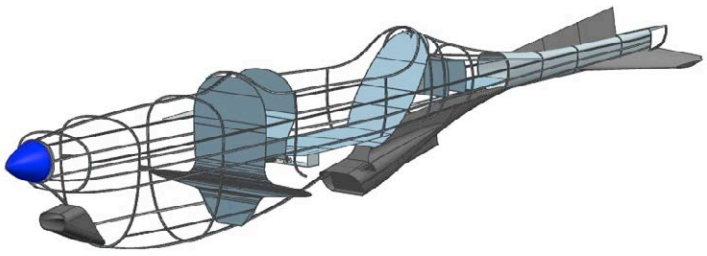

Figure 10-1 : Fuselage Structure

Notice the tail cone is that of full mononcoque structure. Since there is a large weight margin this will be comprised of composite honeycomb.

Due to having a significant weight allowance, the aircraft will be structurally design to surpass the +6g loading as stated by the RFP given by AIAA Reference 1. Given the higher cruise velocity than previous racers, it would acceptable to design the aircraft for +9 g loading (ref. 22).

10.2 Wing Structure

The wing, much like the fuselage, is a semi-monocoque structure. Comprised of ribs to keep the shape of the wing, the surface, or skin, is composite paneling for ease of manufacturing, accessibility and maintenance. As what will be explained in the Fuel System Section, the leading edge will be a "D" shaped frame composed from Kevlar. This is to provide protection from impacts, such as bird strikes, from puncturing the fuel tanks. The main spar located at the quarter chord of the wing will be that of an I-beam structure, while the aft spar, located at 80% chord will be a U-channel beam. As mention previously, all structures within the wing will be composite items. As cost in not of an issue, manufacturing process that provide high surface finish and high precision will be taken in use (ref 22).

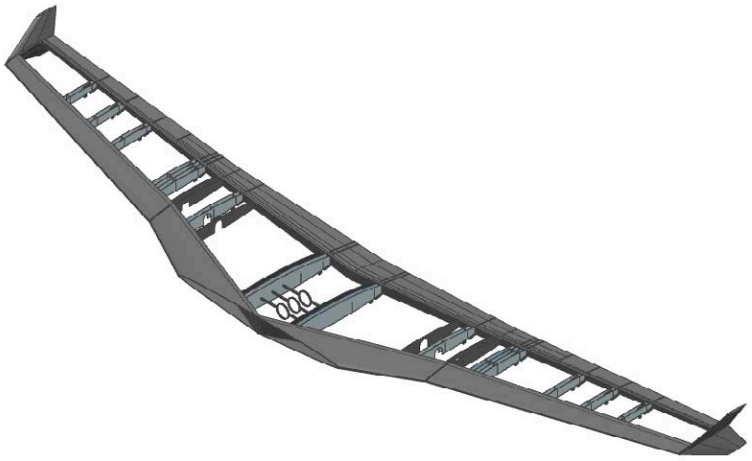

Figure 10-2: Wing and Wing Fence Structure

The wing fences will be a full monocoque construction. As the only need to access the interior of the wing fences would be to install the navigation lights located on the outer tips, accessibility is not of importance. In addition, if there should ever arise a problem to where a wing fence needs to be replaces, a simple quick connection for the navigation lights will be used to allow for a quick turnaround time (ref 22). Shown in the following figure one can see the wing and wing fence structure.

The aileron and flap spars will be at the leading edge as that is the location of its hinge point. The aileron and flap will be that of the same semi-monocoque construction as the wing, using composite ribs to hold the shape of the surfaces and to allow for the skin paneling to attach. See Section 3.3.2.1 for further detail on the integration of the flap and aileron to the wing (ref 22).

10.2.1 Wing-Fuselage Integration

The forward spar of the wing continues into the fuselage to attach to the firewall of the aircraft. This will provide a rigid torque box for the aircraft. In addition at the point where the wing spars protruded into the fuselage, ring frame are placed to transfer the load throughout the airplane (ref 22).

To allow for a smooth transition for the fuselage surface to the wing surface, wing fillets were implemented.

10.3 Horizontal Tail Structure

The horizontal tail is a semi-monocoque structure, just like the wing, using composite ribs and surface paneling skin. The forward spar unites with the forward spar of the vertical tail and the center spar unites with the aft spar of the vertical tail. As the empennage configuration is that of a T-tail, the structural support for the horizontal-vertical tail interface is very rigid.

Shown below are the dispositions of the horizontal tails' spars.

- Forward: .214c, U-beam
- Center: .408c, I-beam
- Aft: .676c, U-channel

The elevator spar located at 1/3 of the elevator chord (ref 22).

10.3.1 Vertical Tail Structure

The vertical tail is exactly like the horizontal tail, semi-monocoque construction, composite ribs and skin surface. Shown below are the dispositions of the vertical tails' spars.

- Forward spar: .25c, U-channel
- Aft Spar: .53c, U-channel

The rudder is exactly like the elevator, with the spar located at 1/3 of the rudder chord (ref 22).

10.4 Engine Integration

The hard points of the engine were determined in Reference 23. These hard points were used to design a substructure for the engine and nose landing gear mounts. The mount will be used to cantilever the engine of the firewall (ref 22).

The engine exhaust will be routed directly from the piston heads out the side of the aircrafts skin, to decrease overall wetted area.

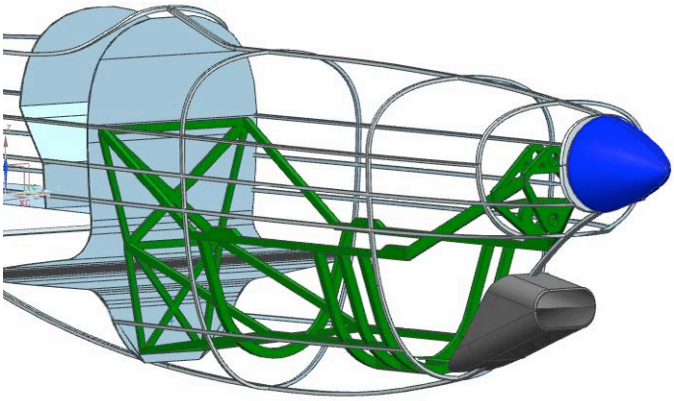

Figure 10-3: Engine Structure

For engine accessibility, maintenance and replacement, the upper half of the engine bay will be removable, allowing for the ease of maintenance and for the complete engine to taken out by a lift (ref 22).

10.5 Dorsal and Ventral Strakes Structure

Both ventral and dorsal strakes will be a fully-monocoque composite structure with a skin thickness 0.03". The dorsal strake will be structurally reinforced as it will be taking torsional loads as seen from the horizontal and vertical tail.

10.6 V-n Diagram

Shown in the figure below one can see the V-n diagram for the Atlas RX

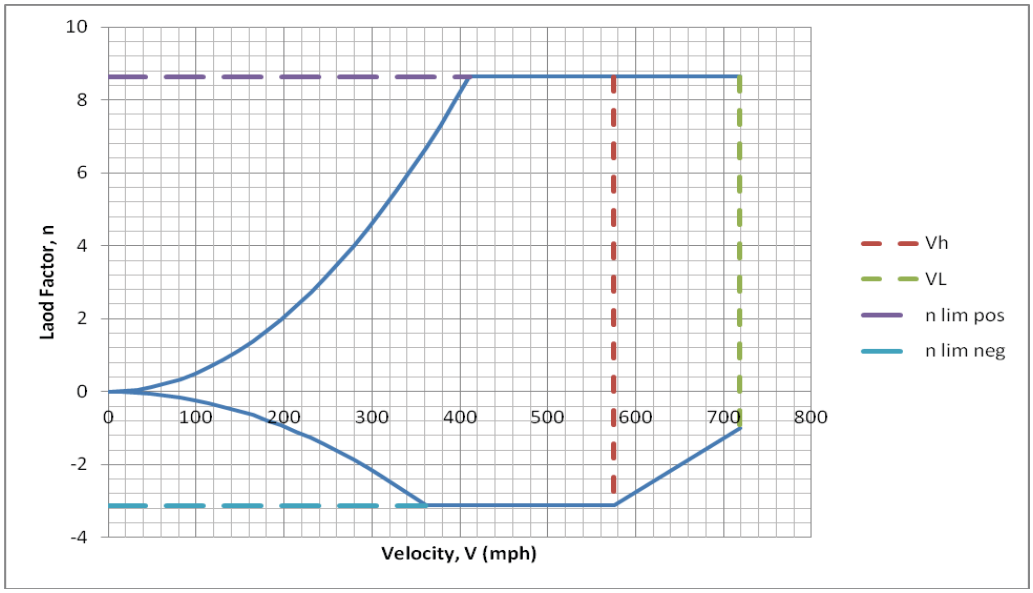

Figure 10-4: Atlas RX V-n Diagram

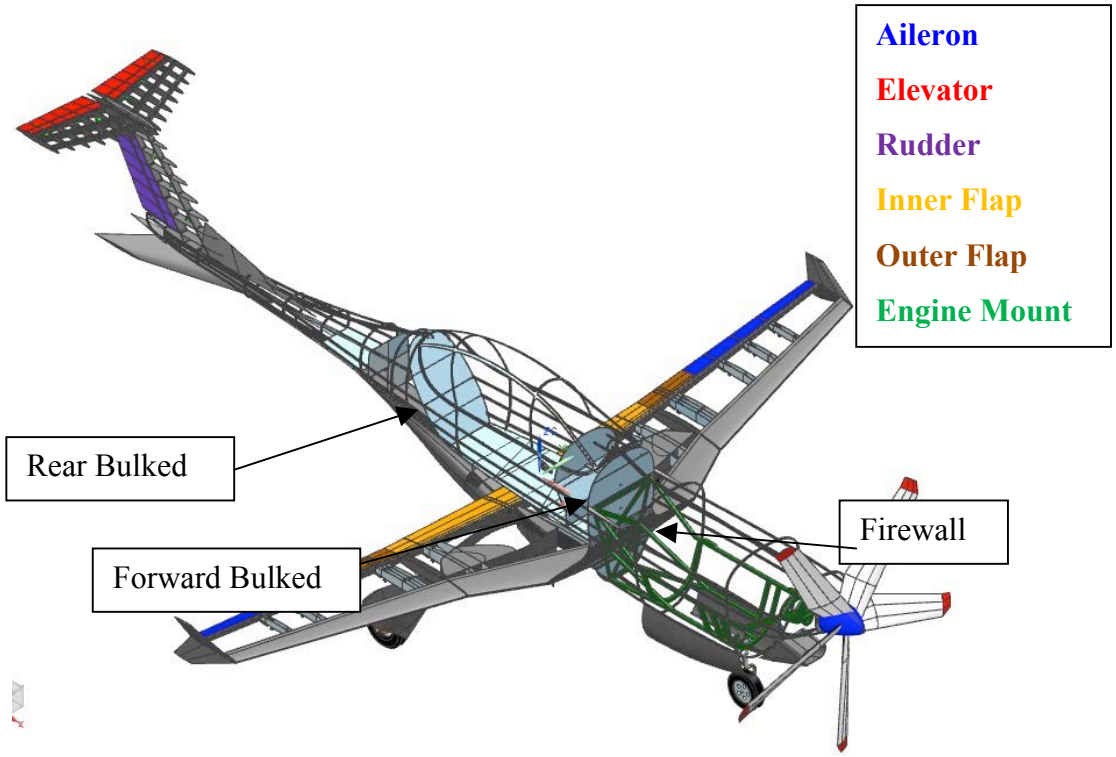

Figure 10-5: Structural Layout

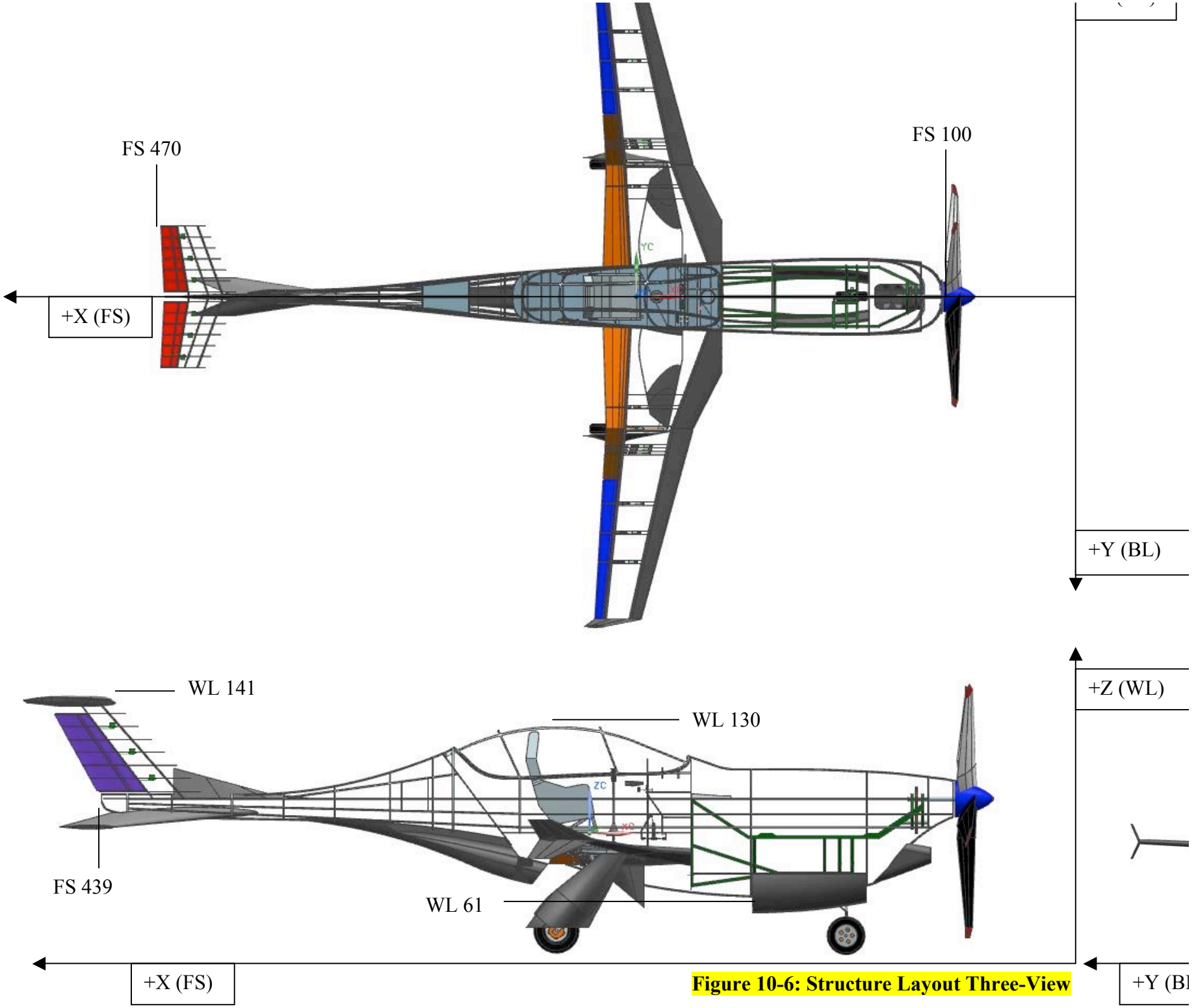

Figure 10-6: Structure Layout Three-View

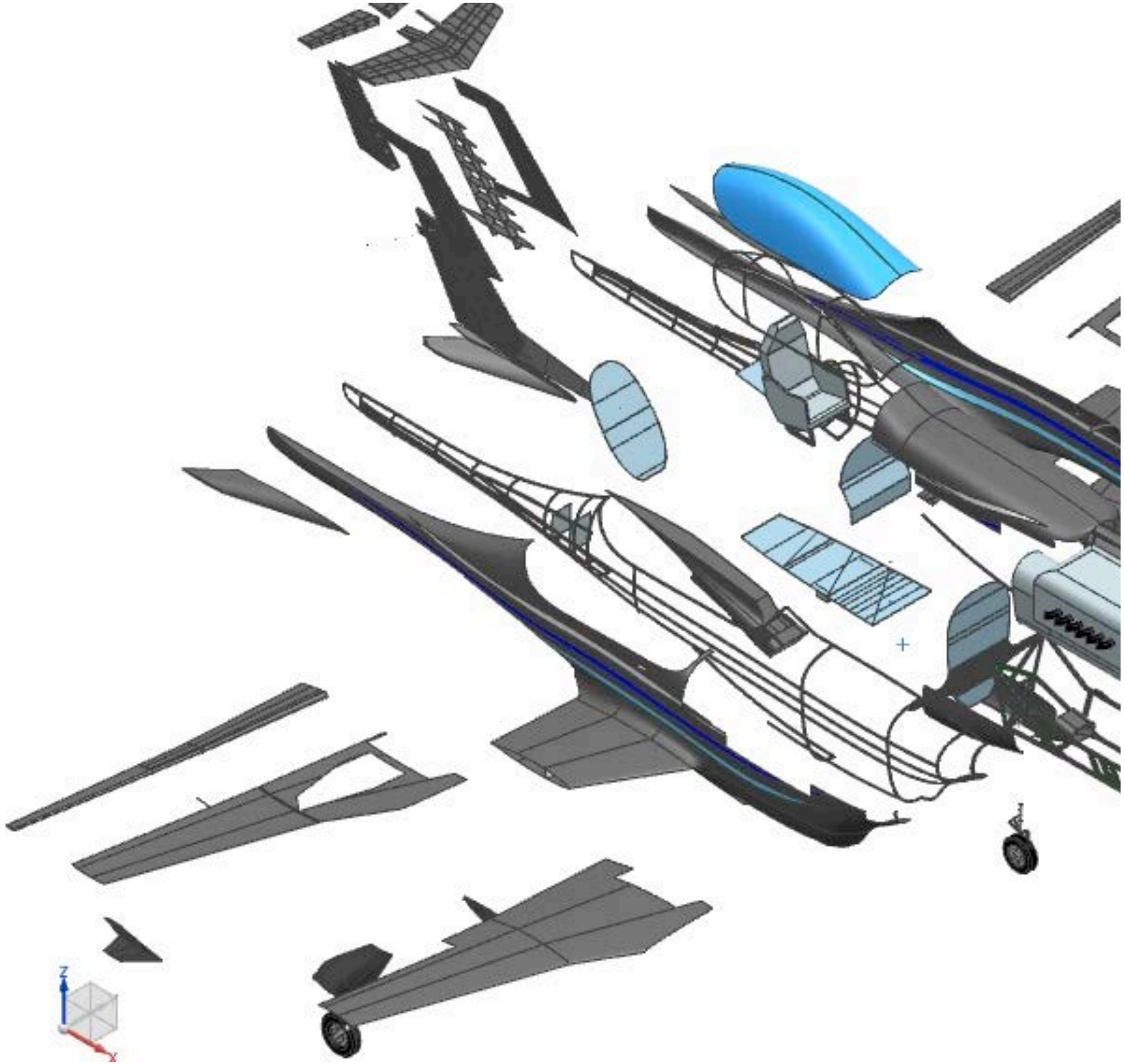

Figure 10.7: Manufacturing Break Down

11 Systems

The control systems for the Atlas RX are as follows;

- Flight control systems
- Fuel systems
- Electrical systems
- Hydraulic systems
- Air-pneumatic systems
- Fire extinguisher
- Environmental
- Visual System

11.1 Description of Flight Control Systems

The flight control system for the Atlas RX is a triple redundant irreversible system. Simply put for every control surface there will be three independent actuators driven from three independent computer systems taking data from three separate potentiometers connected to the devices driven by the pilot. This type of flight control system was chosen to increases reliability of pilot input-actuator output.

The primary flight control systems of the Atlas RX include;

- Ailerons
- Elevator
- Rudder
- Flaps

The secondary flight control system of the Atlas RX includes;

- Power control

11.1.1 Flight Control System 1

Shown in the figure below, one can see a close up view of the flight control system 1, which is located underneath the pilot seat and below the cockpit floor.

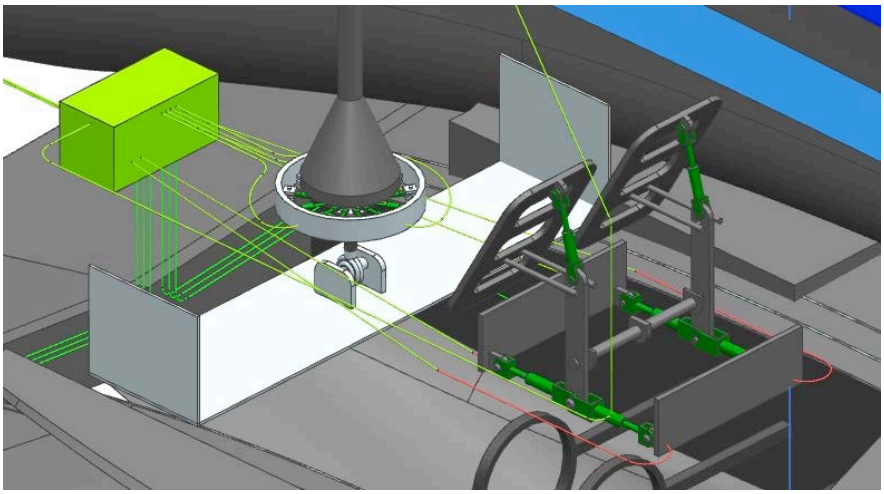

Figure 11-1: Close up view of Flight Control System 1

Shown in the figure below, one can see the flight control system 1 within the aircraft.

Figure 11-2: View of Flight Control System 1 in the Aircraft

11.1.2 Flight Control System 2

Shown in the figure below, one can see a close up view of the flight control system 2, which is located behind the pilot seat and above the cockpit floor.

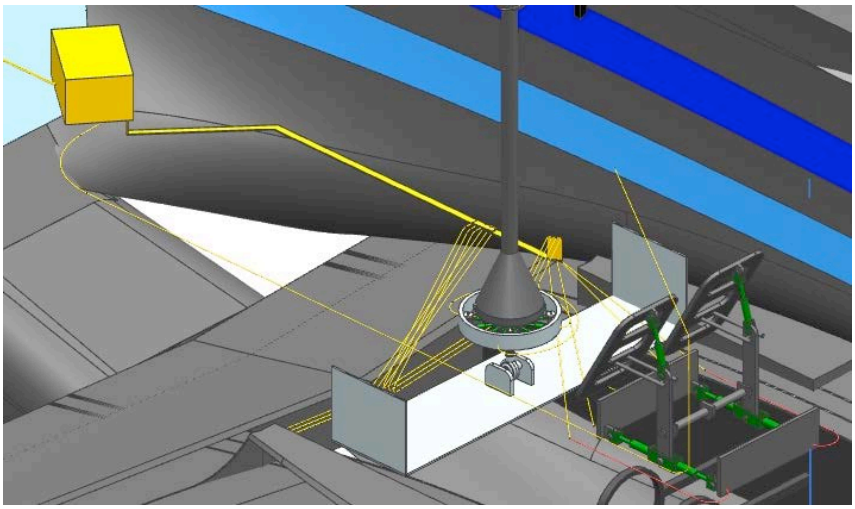

Figure 11-3: Close up view of Flight Control System 2

Shown in the figure below, one can see the flight control system 2 within the aircraft.

Figure 11-4: View of Flight Control System 2 in the Aircraft

11.1.3 Flight Control System 3

Shown in the figure below, one can see a close up view of the flight control system 3, which is located in front of the front panel and above the cockpit floor.

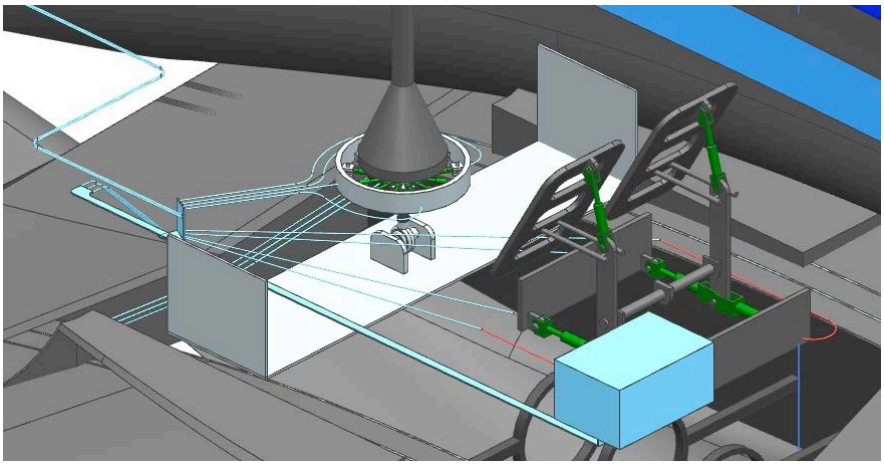

Figure 11-5: Close up view of Flight Control System 3

Shown in the figure below, one can see the flight control system 3 within the aircraft.

Figure 11-6: View of Flight Control System 3 in the Aircraft

11.1.4 Actuator Sizing

To size to actuators for the control surfaces the dynamic pressure on the individual surfaces were found first. Shown in the table below on can see the force needed for each control surface.

Table 11-1: Actuator Sizing

Aileron	1280 lbs
Elevator	953 lbs
Rudder	1150 lbs
Flap	11000 lbs

11.1.5 Power control System

The power control system consists of;

- Throttle
- Mixture
- Propeller pitch
- Starter

To reduce the work load of the pilot the propeller will be that of a collective pitch control propeller. By allowing the pilot control the power rating by a simple lever the propellers pitch and engine mixture will be controlled by the internal flight control systems. Shown in the figure below one can see the power control general arrangement.

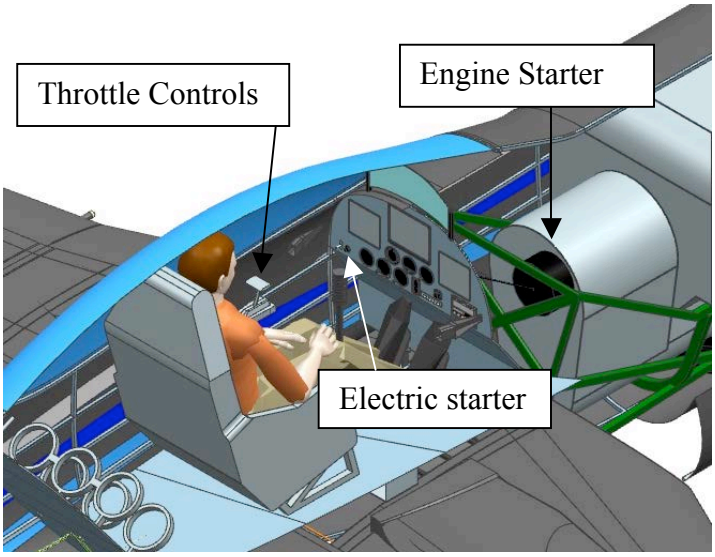

Figure 11-7: Throttle System in Aircraft

11.2 Description of the Fuel System

The fuel system consists of the following;

- Fuel tanks

- Fuel tanks inner bladder
- Air-Pneumatic system for fuel tanks inner bladder
- Fuel lines
- Fuel pump
- Fuel regulator
- Fuel gage

From Reference 10, the calculated fuel weight is that of 310 lbs equaling 47 gallons. The Atlas Rx has two fuel tanks, one in each leading edge wing half, carrying approximately 25 gallons of fuel in each. As the tanks are located within the leading edge of the wing, the need for protecting the tanks from puncture is apparent. Thus it has been decided that the entire leading edge of the wing will be a Kevlar reinforced "D" shaped substructure frame. Because the tanks are located below the fuel injector of the engine, fuel pumps are needed. Each tank has its own pump prior to the fuel lines combining into the main fuel line. The inner bladders used within the tanks are in place of a vent line. Driven by air power, these bladders will be pumped to eliminate all air pockets that may arise within the tanks as the aircraft races around the course. The fuel regulator, located in the main fuel line, is a secondary pump controlled by the cockpit throttle control. A sight gage, located on the instrument panel, will be connected to the each fuel tank. The gage will be driven by the amount of air within the inner fuel tank bladders, thus showing the amount of fuel left with in the each of the fuel tanks (ref 22).
Shown in the figure below, one can see the fuel tanks and pumps.

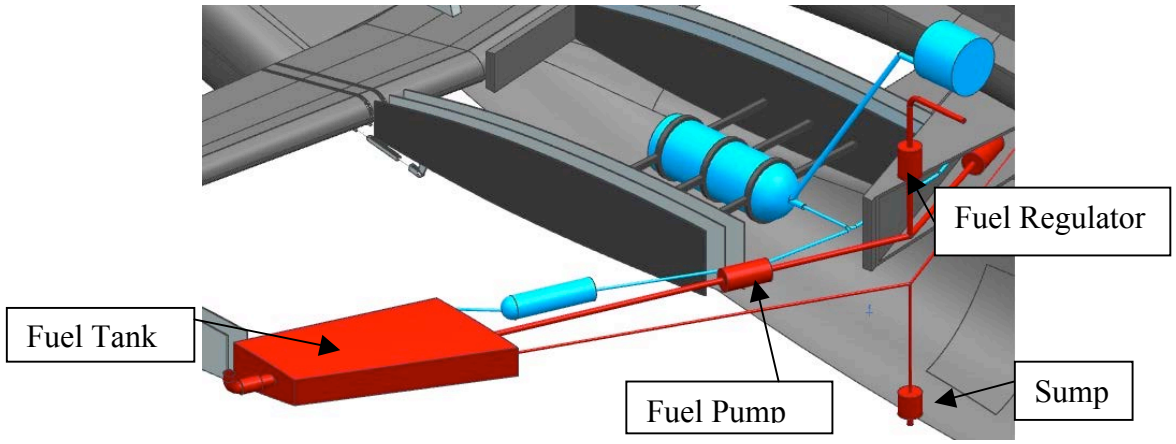

Figure 11-8: Close View of Fuel System

The fuel lines are drawn through the leading edge of the wing, connecting in the center of the fuselage. Sumps are located at the lowest point of each tank as well as a central location within the fuselage. The maximum required amount of fuel can be calculated from the following equation (ref 22).

$$P_{TO} * c_p = 1500hp * .9 \frac{lb}{hp - hr} = 1220 \frac{lbs}{hr} \qquad \text{eqn. 10.1}$$

(Reference 15, Equation 5.2)

Shown in the figure below one can see the entire fuel system and general arrangement.

Figure 11-9: Fuel System in Aircraft

11.3 Description of Electrical System

As the flight control system is an irreversible system, it was decided that all actuators for the flight control system would be electrically driven devices. In addition to the flight control system, other items that are electrically driver include the following;

- Navigation lights
- Avionics equipment
- Engine starter
- Nose wheel steering
- Ground proximity sensors
- Battery

The primary power is generated by an alternator driven by the engine and storing reserve energy in a battery. The secondary power is generated by a battery itself (ref 22).

Wires for the electrical system are routed through the entire aircraft. Avoiding a fire, all wires are kept away from the areas to which the fuel system is located. All wires for the ailerons, flaps and wing navigation lights are routed along the inner volume of the forward and aft wing spars. All rudder, elevator and tail navigation wires are routed through the fuselage tail cone and following aft surface of the leading spars of the horizontal and vertical tails. Shown in the figure below one can see the left wing navigation light (ref 22).

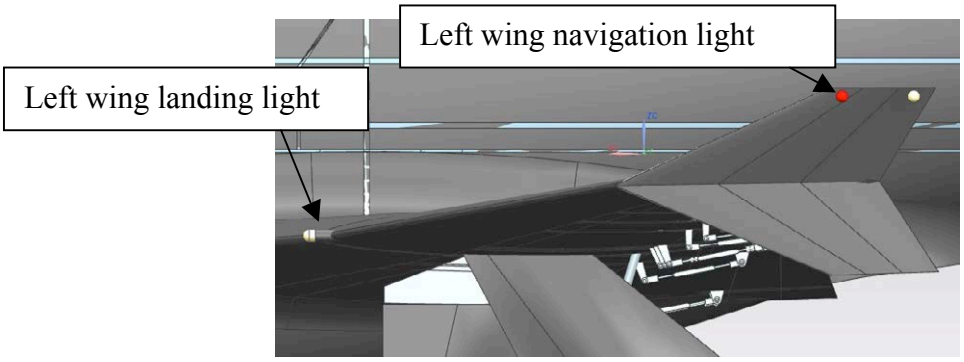

Figure 11-10: Left Navigation Light

To reiterate again, the Atlas RX will have ground proximity sensors, one mounted on each wingtip and the bottom of the fuselage. Refer to section 2.2 Safety, for further detail.

All of the navigation lights' wires come to a central control unit located in the cockpit. Shown in the figure below, one can see the general arrangement of the electrical equipment.

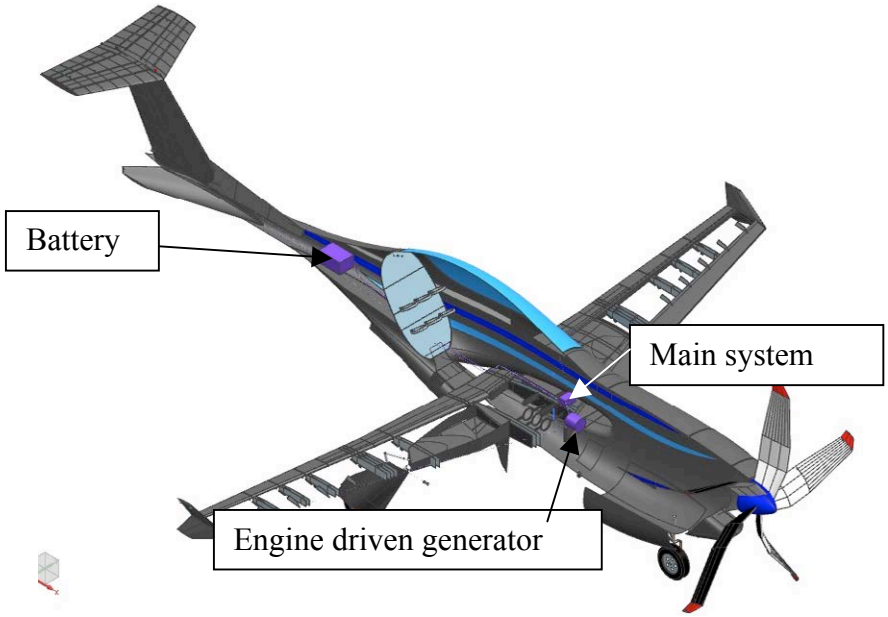

Figure 11-11: Electrical System in Aircraft

11.4 Description of Hydraulic System

The hydraulic system of the Atlas RX is used solely for canopy and landing gear retraction and braking system. System components include;

- Two engine driven pumps
- Reservoir
- Brake disks
- Landing gear retraction/ extension rams
- Landing gear doors
- Canopy
- Ground Stearing

For brake cockpit control a small hydraulic piston is located in conjunction with the rudder foot pedals. From this, lines are routed to a main hydraulic reservoir where finally lines are routed to the each of the brakes located on each wheel axel. Shown in the figure below one can see the brake pedal and piston (ref 22).

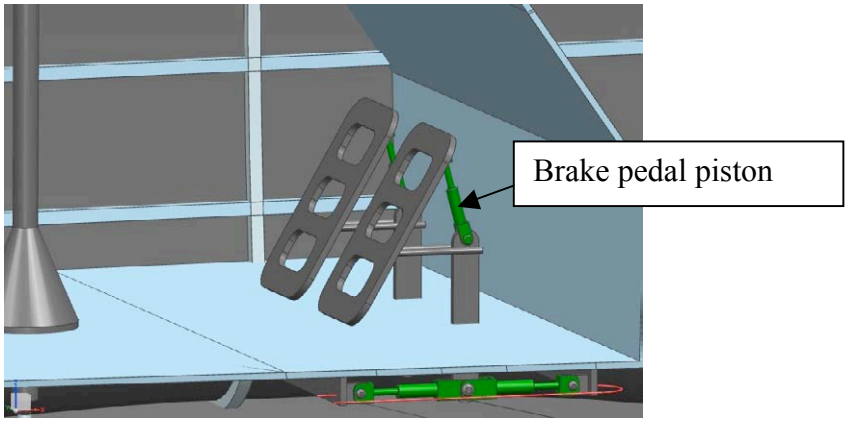

Figure 11-12: Break Pedals and Beak Pistons

Shown in the figure be below one can see one of the landing gear breaking disks.

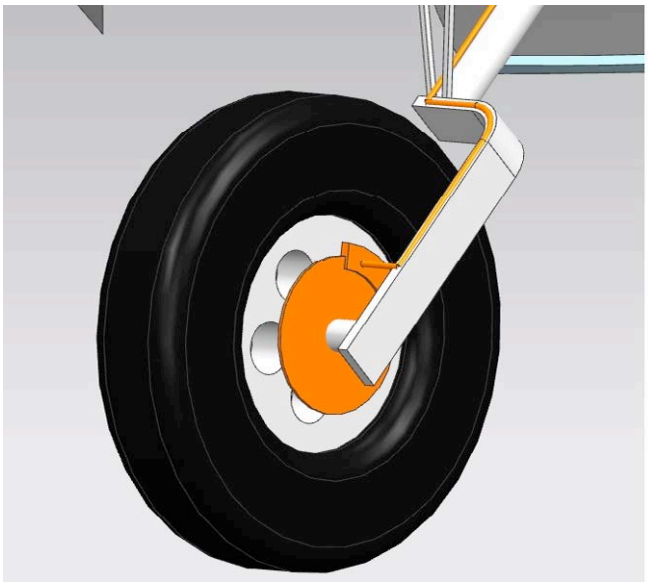

Figure 11-13: Break Disk on Right Main Landing Gear

The landing gear is retracted using hydraulic power. From a switch located in the cockpit, an electrical signal is sent to the hydraulic pump directing fluid to the proper hydraulic pistons thus extending and retracting the landing gear. Shown in the figure below one can see the landing gear extended as well as the open landing gear doors. The outer main landing gear doors do not have any hydraulic rams, as they are mounted directly to the main landing gear struts. Whereas the nose landing gear doors and the inner main landing gear doors are extended and retracted by the hydraulic system (ref 22).

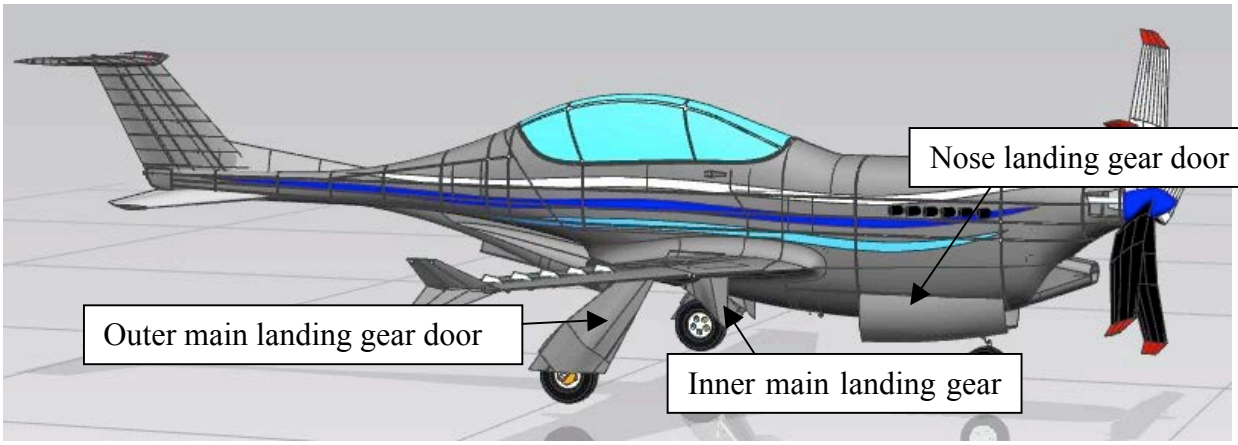

Figure 11-14: Landing Gear Doors

Shown in the figure below one can see landing gear hydraulic rams used to extend and retract the landing gear.

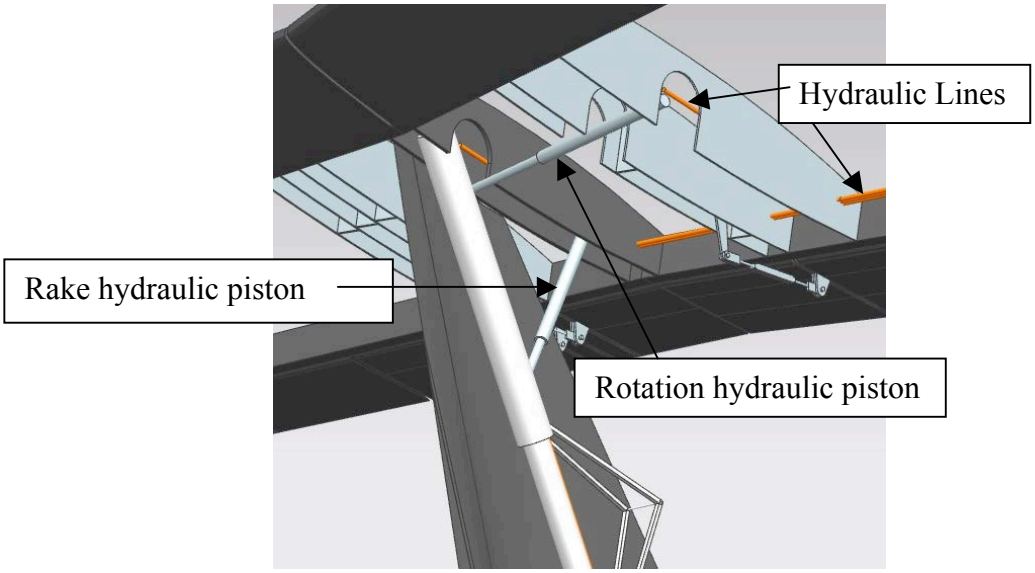

Figure 11-15: Landing Gear Hydraulics

One will notice that there are two hydraulic rams extending each of the main landing gear struts, this is due to storage availabilities and the rake of the landing gear strut.

Because the hydraulic system operates the canopy, brakes and landing retraction, the pressure is assumed to be very high**.** As the brakes do not need a high pressurized system restrictors will be used to reduce the pressure (ref 22). Shown in the figure below one can see the canopy open.

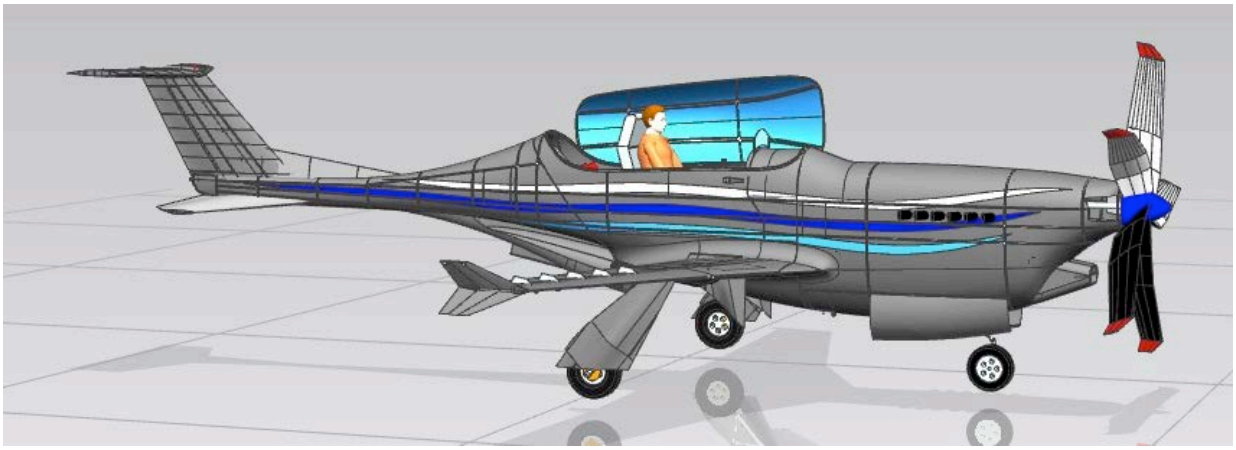

Figure 11-16: Cockpit Open

Shown in the figure below one can see the general arrangement of the hydraulic system.

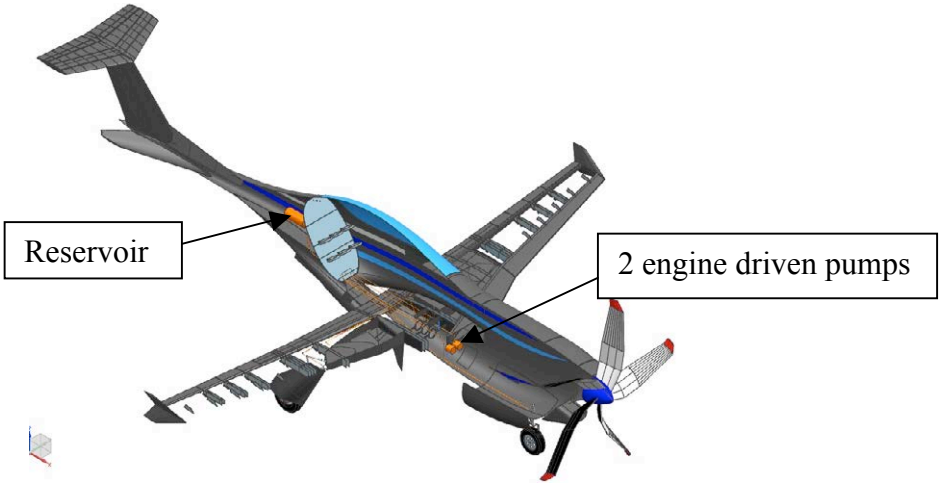

Figure 11-17: Hydraulic System in Aircraft

11.5 Description of Air-Pneumatic System

The pneumatic system consists of solely supporting air for the fuel tank inner bladders. The pneumatic system consists of the following;

- Central air tank
- Engine driven air compressor pump
- Small localized air tanks for each fuel tank inner bladder
- Check valve

Shown in the figure below one can see the general arrangement of the pneumatic system.

Figure 11-18Air-Pneumatic System in Aircraft

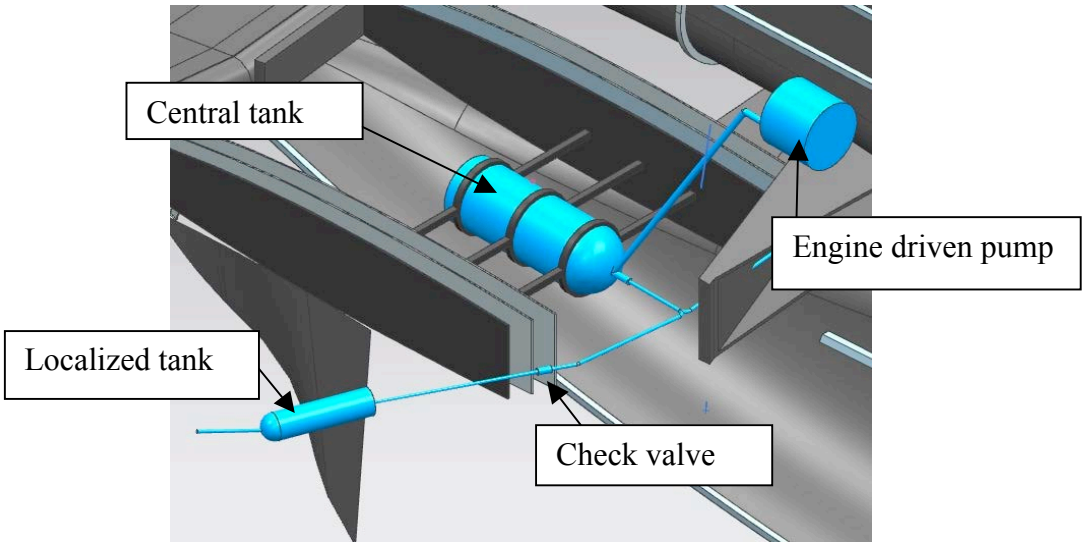

Figure 11-19: Close up View of Pneumatic System

One will notice two check valves, one for each fuel tank. These are in case for whatever reason one of the smaller localized tanks losses air pressure, the larger air tank can still provide the needed air pressure to drive the inner fuel tank bladders (ref 22).

11.6 Fire Extinguisher System

Mention previously, to avoid the same catastrophe that Burt Rutans' Pont Racer experienced, the Atlas RX will employ a fire extinguisher system. Consisting of a pressurized air tank to propel the material within the fire extinguisher tank through the vents, the entire engine bay will be have complete fire extinguishing capability.

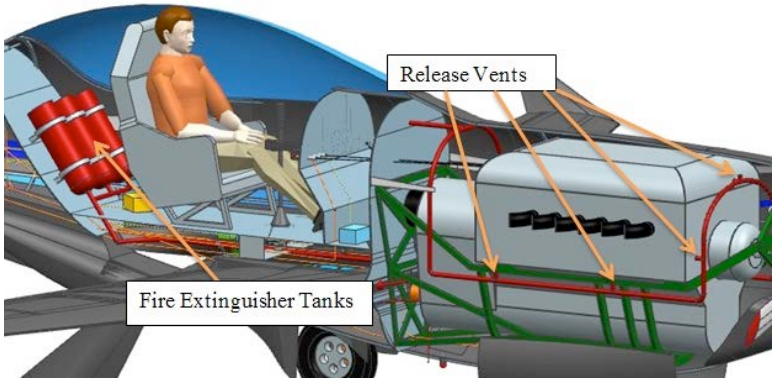

Figure 11-20: Fire Extinguisher System

11.7 Environmental System

To provide cooling to the pilot while racing in Reno's hot summer heat, National Advisory Committee for Aeronautics, NACA, inlets will be used to direct airflow within the cockpit and towards the pilot. Shown in the figure to the right one can see the NACA inlets mounted on the side of the fuselage.

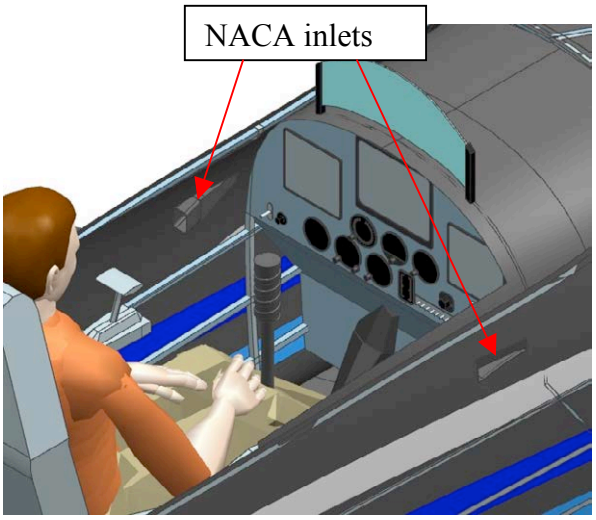

11.8 Visual System

To assist with visibility in the pilots "blind spots," two heads up LCD displays with in the cockpit will allow for a full 360 degree view around all axes. Shown in the figure below one can see the two LCD displays within the cockpit.

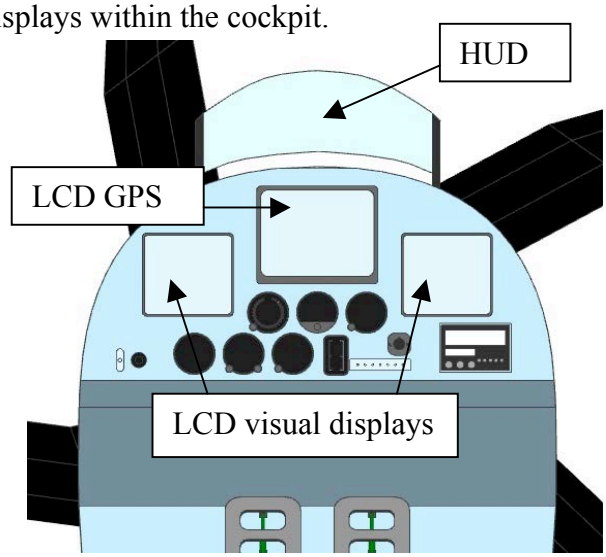

Figure 11-21: Visual Systems, LCD Displays and HUD

11.9 All Systems

Shown in the figure below on can see the general arrangement of all systems.

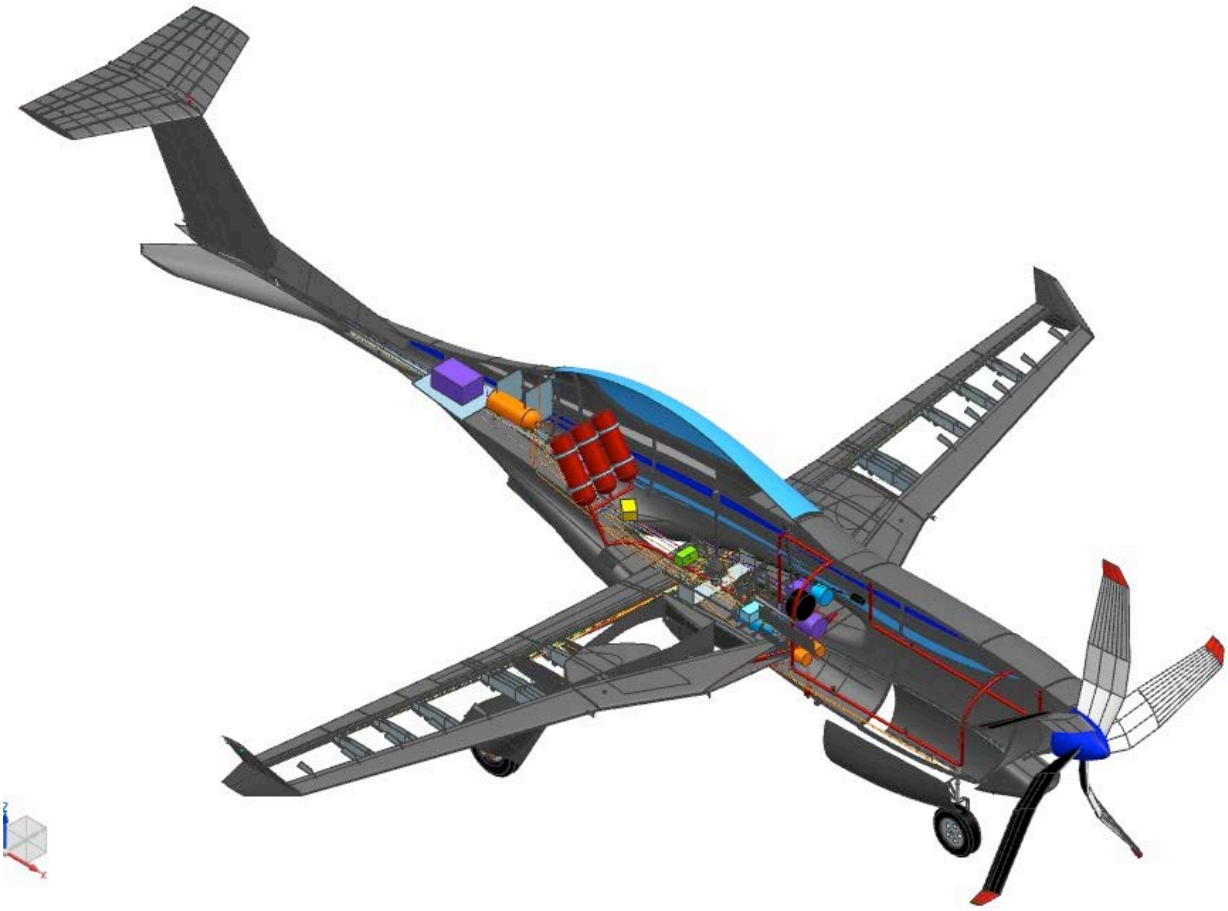

Figure 11-22: General Arrangement of All Systems

12 Advance Technologies

From the first flight at Kitty Hawk, aircraft technology has been ever progressing. Some of the advanced technology the Atlas RX will use, as mentioned previously are the following;

- Artificial vision
- Ground Proximity sensors
- Composite structures
- High impact resistant canopy glass
- Ejection seat

Already being used in Reno Air Races, artificial vision is a true advantage to the pilot. While allowing pilot to focus on what is in their path, the heads up display is of no burden. Not

only does this give the pilot an advantage to plan their flight path, but they will be safer doing it.

Having ground proximity sensors, not only increases the safety factor, but also increases the reliability of the aircraft. Adding this system to the aircraft allows for a higher degree of accuracy within the programming of flight control system.

The technology that we now have in composites and plastics are reaching ever new heights. Though the use of composite structures, doors open to being capable of producing a very light structural frame, allowing for the majority of the weight to be given to other components such as the massive engine. Using Kevlar as a leading edge, will not only protect to fuel tanks, but add to the rigidity of the wing and therefore an overall lighter wing. As mentioned previously, high impact resistant canopy glass will be utilized on the Atlas RX to prevent any debris or flying birds from penetrating the cockpit and injuring the pilot.

Even though ejection seats have been around for decades, the use of them has failed to reach Reno Air Racing. Had this been implemented Jimmy Leeward, pilot of Galloping Ghost, would be alive today. With greater safety precautions this sport that we all love can stay preserved.

Due to the high g loading seen by the aircraft while racing around the track, a g suit is needed to be worn by the pilot. Some of the current suits on the market use compressed air; the one worn by the pilot of the Atlas RX will be a water filled suit. This reason for this is, for whatever reason the pneumatic system should lose pressure, conciseness of the pilot must be preserved. Thus with a water filled suit will be worn as the pressure against the pilot remains constant.

13 Cost Estimations

It is known that initial production cost can be very extreme for a new aircraft. However; this aircraft could be modified to be a military trainer. By adding a second seat with in the cockpit, funding for the racing model, as shown in this report, could be funded by the sales and production of the military trainer version. As this is only a concept, the cost to produce the racing version is found by the following equation;

$$AMP_{1989} = inv\log\left(2.3341 + 1.0586\left(\log W_{TO}\right)\right) \qquad \text{eqn. 12.1}$$

(Reference 24, Equation A13)

$$AMP_{1989} = \$1,781,345.73 \qquad \text{eqn. 12.2}$$

Because of the maneuverability, advanced technology and high precision construction military standards of pricing were used.

Shown in the following table one can see similar aircraft that were analyzed to compare takeoff weight and AMPR weight trend line used to create a trend line.

Make table all on one page

Table 13-1: Takeoff Weight, W_{TO} & AMPR Weight, W_{AMPR} of Comparable Aircraft

	Takeoff Weight, W_{TO} (lbs)	AMPR Weight, W_{AMPR} (lbs)
Nemesis NXT	2600	1400
P-51	12,000	5250
Dago Red	7800	3620
P-51 Strega	8650	3960
Rare Bear F8F-2 Bearcat	8500	3900
Sea Fury FB11	12500	5440
Pond Racer	4140	2090
F6F Hellcat	12600	5480
F7F Tigercat	25700	10100
Super Corsair F2G-2	13300	5740
Spitfire Mk Vb	6620	3140
Hughes H-1 Racer	5500	2670

Gee Bee Model R-1	2415	1320
T-6G Texan	5617	2720
Yak 11	4189	2110
Yak 3	5864	2830
Yak 7	6512	3090
Yak 9U	6858	3240
Yak 9U VK-107	7094	3330
Bell P-39 Aircobra	7379	3450
Atlas Rx	5010	2470

AMPR weight was calculated using the following equation.

$$W_{AMPR} = inv\log\left(0.1936 + 0.8645\left(\log W_{TO}\right)\right)$$ eqn. 12.2

(Reference 24, Equation 3.5)

Shown in the following figure one can see the chart showing takeoff weight, WTO, vs. AMPR weight, WAMPR, along with a trend line and trend line equation.

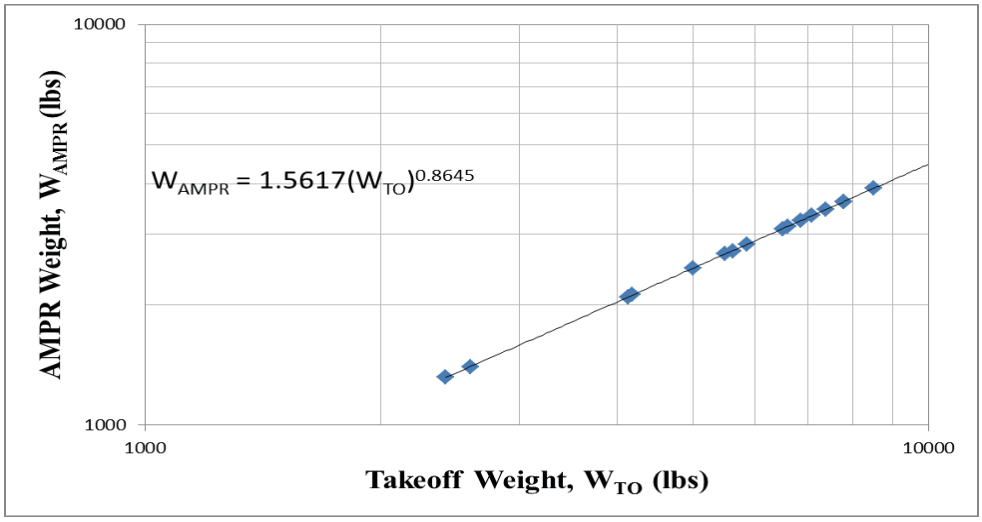

Figure 13-1: Takeoff Weight, W_{TO} & AMPR Weight, W_{AMPR} of Comparable Aircraft

Reference

1. Anon., "2011-2012 AIAA Foundation Undergraduate Individual Aircraft Design Competition," *American Institute of Aeronautics and Astronautics (AIAA), AIAA Website* [http://www.aiaa.org} AIAA, Reston, Virginia, 30, August 2011, 4:20 pm.
2. Anon., " NX Software," *Siemens Product Lifecycle Management Software Inc*., Version 7.50.32, Plano, TX, 2009
3. Anon., "Advanced Aircraft Analysis Code," *DARcorp Computer Software,* Version 3.3, Lawrence, KS, 2011.
4. Anon., "Voodoo," *Air Venture, Air Venture Web Site* [http://www.airventure.de/reno06_5_unl_engl.htm] 13 December 2011.
5. Anon., "Dago Red," *Adrenaline X Racing, Adrenaline X Racing Web Site* [http://forum.adrenalinex.co.uk/index.php?topic=2220.135] Adrenaline X Racing, 13 December 2011.
6. Anon., " Rare Bear," *DB Mueller Fine Art, DB Mueller Fine Art Web Site* [http://dbmueller.com/racers/] DB Mueller Fine Art, 13 December 2011, 12:28 pm.
7. Anon., "Galloping Ghost Specifications," *RAF Group 45, LLC, Leeward Air Ranch Racing Team Web Site* [http://www2.leewardairranch.com/racing/galloping-ghost-specs] RAF Group 45, LLC, 13 December 2011, 12:56 pm.
8. Anon., "US16E-JSF Ejection Seat," *Martin Baker Aircraft Company Limited, Martin Baker Web Site* [http://www.martin-baker.com/products/Ejection-Seats/Mk--16-high-speed/US16E---JSF.aspx], Martin Baker Aircraft Company Limited, 13 December 2011, 1:43 pm.
9. Anon., "Reno/Stead Airport," *Reno Stead Airport*, *Wikipedia Website* [http://en.wikipedia.org/wiki/Reno_Stead_Airport] 15, September 2012, 1:40 pm.
10. Lopez, Alex, "AE 721 Design Report Number 1: Mission Weight Sizing, Takeoff Weight Sensitivities and Performance Constraint Analysis for the Atlas RX Racer," University of Kansas, Lawrence Kansas, 11 September 2011.
11. Morrison, Jr. W.D., " Advanced Airfoil design Emperically Based Tansonic Aircrft-Drag Buildup Technigue," Lockheed-California Company, Burbank, California, January 1976.
12. Roskam, Jan., *Airplane Design Part II: Preliminary Configuration and Integration of the Propulsion System*, DARcoporation, Lawrence, KS, 2004.
13. Anon., "Specifications," Rolls-Royce Merlin, *Wikipedia Website* [http://en.wikipedia.org/wiki/Rolls-Royce_Merlin] 25, September 2011, 3:40 pm.
14. Roskam, Jan., *Airplane Design Part I: Preliminary Sizing of Airplanes*, DARcoporation, Lawrence, KS, 2008.
15. Roskam, Jan., *Airplane Design Part VI: Preliminary Calculations of Aerodynamics, Thrust and Power Characteristics*, DARcoporation, Lawrence, KS, 2008.
16. Roskam, Jan., *Airplane Design Part IV: Preliminary Layout of Landing Gear and Systems*, DARcoporation, Lawrence, KS, 2007.
17. Anon., " Navigation Light," *Aircraft Spruce & Specialty Co. Aircraft Spruce Web Site* [http://www.aircraftspruce.com/menus/el/winglights.html], Aircraft Spruce, Corona, California 92880, 13 December 2011, 5:18 pm.
18. Anon., " Eletorhydraulic Valve Actuatiors and Hydraulic Valve Actuators from Rotek plc," *GlobalSpec. Inc., GlobalSpec Web Site* Lopez, [http://www.globalspec.com/SpecSearch/Products?Comp=2389&QID=22035749&VID=91991] GlobalSpec. East Greesbush, NY 12061, 13 December 2011, 8:23 pm.
19. Roskam, Jan., *Airplane Design Part VII: Determination of Stability, Control and Performance Characteristics: FAR and Military Requirements*, DARcoporation, Lawrence, KS, 2006.

20. Anon., "The Race Course," *Reno Air Racing Association, Reno Air Racing Association Web Site* [http://www.airrace.org/at_the_races/course.php] Reno Air Racing Association, Reno, Nevada 89503, 15 December 2011, 5:22 pm.
21. Anon., "2011 Qualifying and Race Records," *Reno Air Racing Association, Reno Air Racing Association Web Site* [http://reports.airrace.org/2011/2011.ExistingRecords.Report.html] Reno Air Racing Association, Reno, Nevada 89503, 15 December 2011, 5:40 pm.
22. Alex, "AE 721 Design Report Number 5: Description of Major Systems, Class II Sizing of Landing Gear, Initial Structural Layout, V-n Diagram, Class II Weight and Balance and Updated 3-View for the: Atlas RX Racer," University of Kansas, Lawrence Kansas, 30 November 2011.
23. Lopez, Alex, "AE 721 Design Report Number 2: Configuration Selection, Cockpit Layout, Engine Installation and High Lift Devise Sizing and Wing layout Design for the: Atlas RX Racer," University of Kansas, Lawrence Kansas, 2 October, 2011.
24. Roskam, Jan., *Airplane Design Part VIII: Airplane Cost Estimation: Design, Development, Manufacturing and Operating*, DARcoporation, Lawrence, KS, 2006.